Acta Cryst E CRYSTALLOGRAPHIC COMMUNICATIONS

ISSN 2056-9890

Dibasic 3,3′-dinitro-4,4′-bipyrazole-1,1′-diides of K, Rb and Cs reveal metal-selective ring–π over ring–N coordination

Kostiantyn V. Domasevitch* and Vira V. Ponomarova

Inorganic Chemistry Department, National Taras Shevchenko University of Kyiv, Volodymyrska Str. 64/13, 01601 Kyiv, Ukraine. *Correspondence e-mail: dk@univ.kiev.ua

Received 16 April 2026
Accepted 12 May 2026

Edited by W. T. A. Harrison, University of Aberdeen, United Kingdom

Keywords: crystal structure; potassium; rubidium; caesium; nitropyrazoles; ionic pyrazolates; cation–π interaction.

CCDC references: 2553747; 2553746; 2553745

Supporting information: this article has supporting information at journals.iucr.org/e

Three new alkali metal pyrazolate salts, namely, poly[[μ-3,3′-dinitro-4,4′-bipyrazole-1,1′-diido]dipotassium], $[K_2(C_6H_2N_6O_4)]_n$, (**1**), its rubidium analogue $[Rb_2(C_6H_2N_6O_4)]_n$, (**2**), and poly[[[μ-3,3′-dinitro-4,4′-bipyrazole-1,1′-diido]-dicaesium] monohydrate], $\{[Cs_2(C_6H_2N_6O_4)]\cdot H_2O\}_n$, (**3**), suggest that the electron-depleted nitropyrazolates may be still functional as efficient π-donors toward late alkali metal ions. The three-dimensional structures of **1** and **2** are very similar, being governed by μ_4-κ^1:κ^1:κ^1:κ^1 coordination of the pyrazolate anions as hard Lewis bases [K—N = 2.783 (3)–2.956 (3); Rb—N = 2.930 (4)–3.194 (4) Å]. In contrast, the structure of **3** reveals a dominant significance for the pyrazolate–π coordination, which produces two distinct motifs in the forms of finite Cs—π arrangement [Cs—ring centroid distance = 3.389 (3) Å] and one-dimensional —Cs—(π—Cs)$_n$— sandwiches with slightly larger Cs—π separations at 3.474 (3) and 3.587 (3) Å. Weaker ion–dipole interactions with the nitro-O donors, at the distances approaching the sums of corresponding ionic radii, are relevant for the entire series and they complete typically high coordination numbers of the metal ions [CN = 8, 9]. These findings may find use in the construction of ion-selective receptors since the existing examples for the coordinative discrimination of the late alkali metal ions, beyond the ion-cavity size match considerations, are still rare.

1. Chemical context

The crystal chemistry of alkali metals azolates (deprotonated five-membered aromatic nitrogen heterocycles with one or more N atoms) provides appropriate models and paradigms for assessing the significance of cation–π interactions, which are energetically superior to the other kinds of aromatic bonding and are applicable for control of solid-state architecture (Yamada, 2020). The cation–π bonding essentially expands the relatively scarce coordination landscape of alkali metal ions (Fabbrizzi, 2020), being a valuable factor for differentiation of their coordination behavior and enabling the construction of artificial ion-selective receptors. The relevance of such interactions to biology is also well established, in particular for mediating high K^+-selectivity of biological ion channels (Dougherty, 2025).

For the most favorable case of electron-rich pyrrolate species, the relatively strong cation–π interactions are likely less sensitive to the nature of cation and they are frequently observed for any of the alkali metals [Li to Cs; Blanco *et al.*, 2008]. That is contrary to polynitrogen azolate anions, *e.g.* pyrazolates, whose propensity for π-bonding is often hidden in the shade of their more competitive interactions as efficient multiple N–σ donors. Theoretical studies of Li, Na and K pyrazolates reveal that *M*—N coordination is the most

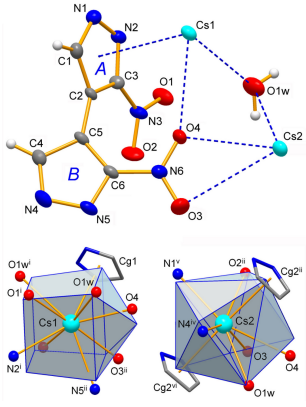

favorable. Although in the case of Na and K two alternative structures are closer in stability (Cortés-Llamas *et al.*, 2006), all *M*–π-pyrazolate configurations spontaneously revert to the more stable N–σ ones (Blanco *et al.*, 2008). This may be attributed not only to the increased number of such donor-N sites, but also to the essential decrease in π-electron density upon the accumulation of endocyclic N atoms. A similar impact for bonding preferences comes from the incorporation of an appropriately strong acceptor. In this way, the computational models of Na^+-nitrobenzene pairs suggest a total destabilization of the configurations involving Na^+ at the π-cloud (Watt *et al.*, 2009). The combination of these co-aligned factors in the case of nitropyrazolates evidently mitigates against π-coordination, but such destructive impact could be fatal primarily for the harder Lewis acids (Li^+, Na^+, K^+). The late alkali metal ions are prone to support contacts with delocalized and diffuse electron densities over coordinating the centers of highest charge and therefore, in this case, the *M*–π coordination may be more tolerant to the π-electron depletion. One can postulate essential selectivity for *M*–π over *M*–σ-N coordination, depending on the Lewis hardness/softness of the metal ion. For example, while the crystal chemistry of Na and K phenolates is dominated by *M*—O coordination, Cs compounds exhibit more complex, if not a completely different, behavior with only a few Cs—O interactions accompanying the multiple π-coordination patterns (Pink & Sieler, 2007).

Keeping in mind these inputs, we have examined the K^+, Rb^+ and Cs^+ salts of 3,3′-dinitro-4,4′-bipyrazole (**1**–**3**, respectively) and report their structures here.

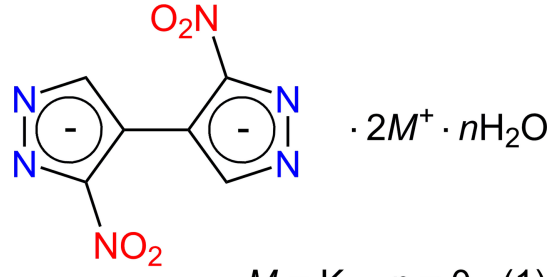

M = K, *n* = 0 (1)

M = Rb, *n* = 0 (2)

M = Cs, *n* = 1 (3)

2. Structural commentary

The molecular structures of the title compounds **1**–**3** are shown in Figs. 1–3, respectively. They represent similar dibasic salts, with the metal ions and organic dianions found in 2:1

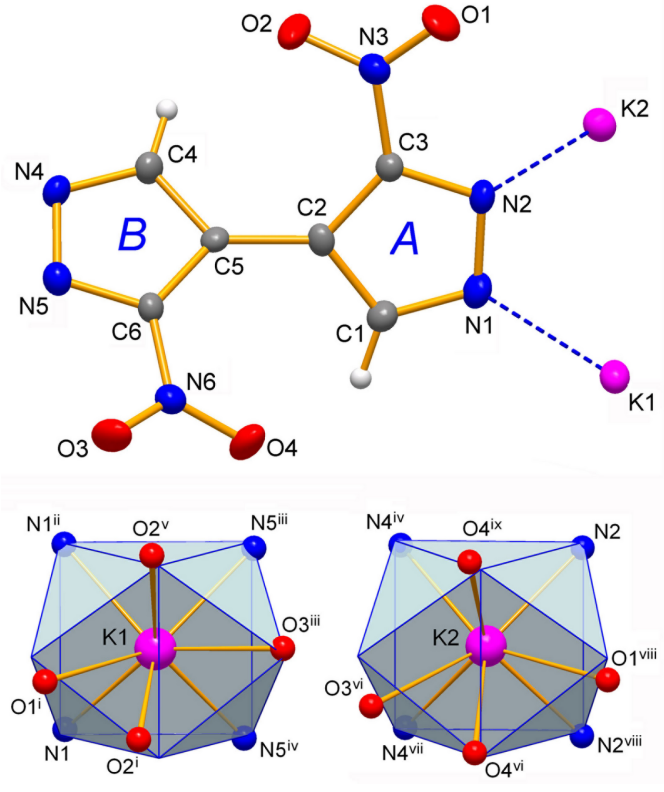

Figure 1
The molecular structure of **1** with displacement ellipsoids at the 50% probability level. The coordination environments of two K ions are drawn against the best fitted idealized polyhedra in the form of biaugmented trigonal prisms. For symmetry codes, see Table 1.

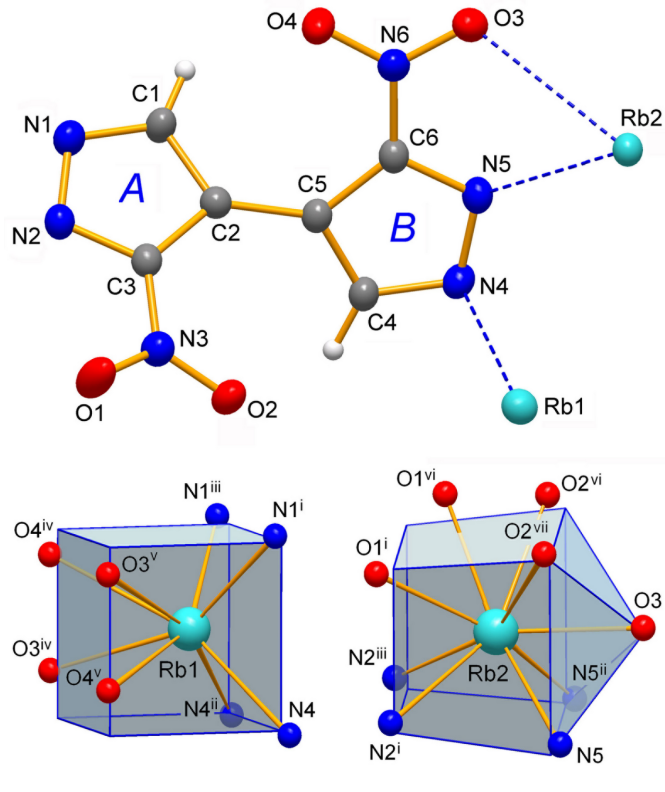

Figure 2
The molecular structure of **2** with displacement ellipsoids at the 50% probability level. The coordination environments of two metal ions are drawn against the best fitted idealized polyhedra in the form of cube (Rb1) and spherical-relaxed capped cube (Rb2). For symmetry codes, see Table 2.

Table 1
Selected bond lengths (Å) for **1**.

K1—O2^{i}	2.719 (2)	K2—O4^{vi}	2.853 (2)
K1—N1^{ii}	2.783 (3)	K2—N2	2.859 (3)
K1—O3^{iii}	2.795 (2)	K2—N4^{vii}	2.901 (3)
K1—N5^{iii}	2.828 (3)	K2—N2^{viii}	2.917 (3)
K1—N5^{iv}	2.850 (3)	K2—O1^{viii}	2.945 (2)
K1—N1	2.871 (3)	K2—N4^{iv}	2.956 (3)
K1—O1^{i}	3.091 (3)	K2—O4^{ix}	2.973 (3)
K1—O2^{v}	3.418 (3)	K2—O3^{vi}	3.153 (2)

Symmetry codes: (i) $-x+\frac{1}{2}, y, z-\frac{1}{2}$; (ii) $x, y-1, z$; (iii) $x+\frac{1}{2}, -y-1, z$; (iv) $x+\frac{1}{2}, -y, z$; (v) $-x+\frac{1}{2}, y-1, z-\frac{1}{2}$; (vi) $-x+\frac{1}{2}, y+1, z+\frac{1}{2}$; (vii) $x+\frac{1}{2}, -y+1, z$; (viii) $x, y+1, z$; (ix) $-x+\frac{1}{2}, y, z+\frac{1}{2}$.

proportions, and accommodating also one solvate water molecule in the case of **3** [*M* = Cs]. The ease of crystallization of such salts from alkaline aqueous solutions is governed by the appreciable acidity of nitro substituted pyrazoles, which are weak NH acids comparable to phenols [pK_a = 9.81 for 3(5)-nitropyrazole *versus* 14.63 for the parent pyrazole; Janssen *et al.*, 1973].

The bonding preferences of K^+ and Rb^+ ions are very similar. They adopt typically high coordinations with four pyrazolate-N atoms complemented by four (or five for Rb2 in

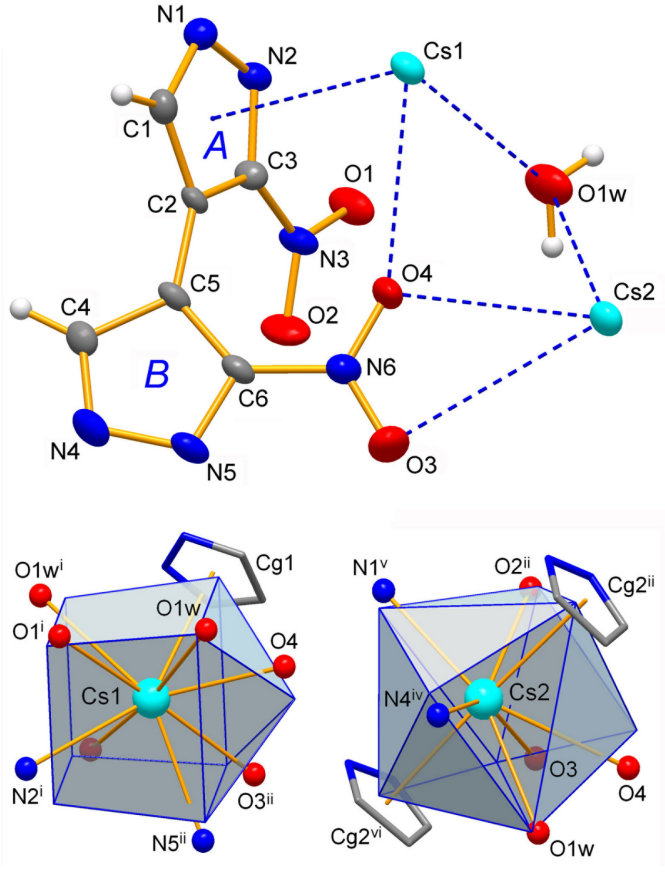

Figure 3
The molecular structure of **3** with displacement ellipsoids at the 50% probability level. The coordination environments of two metal ions are drawn against the best fitted idealized polyhedra in the form of spherical-relaxed capped cube (Cs1) and triangular dodecahedron (Cs2) and when considering only the closest N1^{v} atom for κ^2-coordinated pyrazolate group in the case of Cs2. For symmetry codes, see Table 3.

Table 2
Selected bond lengths (Å) for **2**.

Rb1—N1^{i}	2.930 (4)	Rb2—O1^{vi}	2.993 (4)
Rb1—N4^{ii}	2.980 (4)	Rb2—O3	3.004 (4)
Rb1—N1^{iii}	2.987 (4)	Rb2—N5	3.016 (4)
Rb1—N4	3.088 (4)	Rb2—N5^{ii}	3.017 (4)
Rb1—O3^{iv}	3.103 (4)	Rb2—N2^{iii}	3.101 (4)
Rb1—O3^{v}	3.113 (4)	Rb2—O2^{vi}	3.150 (4)
Rb1—O4^{iv}	3.175 (4)	Rb2—N2^{i}	3.194 (4)
Rb1—O4^{v}	3.370 (5)	Rb2—O2^{vii}	3.214 (4)
Rb2—O1^{i}	2.893 (4)		

Symmetry codes: (i) $x-\frac{1}{2}, -y+\frac{1}{2}, z-\frac{1}{2}$; (ii) $x+1, y, z$; (iii) $x+\frac{1}{2}, -y+\frac{1}{2}, z-\frac{1}{2}$; (iv) $-x+\frac{3}{2}, y-\frac{1}{2}, -z+\frac{1}{2}$; (v) $-x+\frac{1}{2}, y-\frac{1}{2}, -z+\frac{1}{2}$; (vi) $-x+\frac{3}{2}, y+\frac{1}{2}, -z+\frac{1}{2}$; (vii) $-x+\frac{1}{2}, y+\frac{1}{2}, -z+\frac{1}{2}$.

Table 3
Selected bond lengths (Å) for **3**.

Cs1—O1^{i}	3.064 (5)	Cs2—O2^{ii}	3.107 (5)
Cs1—O3^{ii}	3.101 (6)	Cs2—N4^{iv}	3.132 (5)
Cs1—O4	3.123 (5)	Cs2—N1^{v}	3.251 (6)
Cs1—O1^{iii}	3.130 (6)	Cs2—O4	3.350 (5)
Cs1—O1*W*	3.215 (6)	Cs2—O1*W*	3.496 (7)
Cs1—N2^{i}	3.273 (5)	Cs2—O3	3.502 (6)
Cs1—N5^{ii}	3.392 (6)	Cs2—*Cg*2^{ii}	3.474 (3)
Cs1—*Cg*1	3.389 (3)	Cs2—*Cg*2^{vi}	3.587 (3)
Cs1—O1*W*^{i}	3.754 (7)		

Symmetry codes: (i) $-x+1, y-\frac{1}{2}, -z+2$; (ii) $-x, y-\frac{1}{2}, -z+1$; (iii) $x, y-1, z$; (iv) $x+1, y, z$; (v) $x, y, z-1$; (vi) $-x, y+\frac{1}{2}, -z+1$.

2) nitro-O atoms at distances that approach the sums of the corresponding ionic radii for eight-coordinate environments [which are *M*—N = 2.97 and 3.07 Å; *M*—O = 2.89 and 2.99 Å for K and Rb ions, respectively; Shannon, 1976]. However, some of the *M*—O bonds are essentially elongated indicating the weakness of these relatively distal ion–dipole interactions (Tables 1 and 2). One can find their median lengths (K—O = 2.96 Å; Rb—O = 3.11 Å) slightly exceeding the above sums of ionic radii whereas the situation for the *M*—N bonding is the reverse (median values for K—N = 2.86 Å; Rb—N = 3.02 Å). The latter could be regarded as a perceptibly stronger and dominant interaction in the structures, as is anticipated for the relatively hard Lewis acid (M^+) and base (pyrazolate-N^-) duo. For comparison, without contribution from *M*—O interactions in homoleptic $[K(Me_2pz)]_n$ [Me_2pz is 3,5-dimethylpyrazolate] the lengths of the K—N bonds fall into the range of 2.79 (1)–2.98 (2) Å (Woods, 2016), which exactly matches the corresponding parameters for **1**. The polyhedral geometries of the K ions in **1** represent similar biaugmented trigonal prisms with the appropriate shape measures of 2.454 (K1) and 3.153 (K2) (Ruiz-Martínez *et al.*, 2008), whereas in the case of the Rb ion in **2**, these are close to a cube [Rb1, CN = 8] and spherical-relaxed capped cube [Rb2, CN = 9] (shape measures are 3.550 and 5.112, respectively) (Figs. 1 and 2).

The bonding of the softer Lewis acid Cs^+ is markedly different (Table 3) and these cations in **3** tend to reside at the π-clouds of the rings [Cs1—(ring *A*); Cs2—(ring *B*)^{ii} and Cs2—(ring *B*)^{vi}; symmetry codes: (ii) $-x, y-\frac{1}{2}, -z+1$; (vi) $-x, y+\frac{1}{2}, -z+1$] (Fig. 3), while supporting a set of relatively distal contacts with either N- or C-atoms over coordinating the centers of highest charge only, seen for **1** and **2**. Moreover, in the case of the Cs2—(ring *A*)^{v} pair, both Cs—N contacts are comparable in length [Cs2—N1^{v} = 3.251 (4) Å; Cs2—N2^{v} =

Table 4
Geometry of the Cs–π-pyrazolate coordination in **3** (Å, °).

Cs···Plane is the distance from the metal ion to the mean plane of the ring and sa is the slippage angle, *i.e.* the angle of the Cs···*Cg* axis to the plane normal.

Ion	Group	Cs—N	Cs—C	Mean Cs—C,*N*	Cs···*Cg*	Cs···Plane	sa
Cs1	(N1/N2/C1–3)	3.433 (4), 3.562 (4)	3.514 (5)–3.703 (4)	3.581 (5)	3.389 (3)	3.360 (2)	7.5 (3)
Cs2	(N4/N5/C4–6)^{ii}	3.442 (5), 3.589 (6)	3.588 (5)–3.868 (5)	3.661 (6)	3.474 (3)	3.406 (3)	11.4 (4)
	(N4/N5/C4–6)^{vi}	3.451 (6), 3.896 (5)	3.448 (6)–4.111 (5)	3.762 (6)	3.587 (3)	3.369 (5)	20.1 (4)

Symmetry codes: (ii) $-x, y-\frac{1}{2}, -z+1$; (vi) $-x, y+\frac{1}{2}, -z+1$.

3.490 (4) Å; symmetry code (v) $x, y, z-1$] and this suggests κ^2-coordination. Such behavior results in partial elimination of Cs—N bonding in favor of new structure-directing interactions, namely cation–π bonds (Table 4). This parallels structural trends for M—π over M—N bonding in metallated porphyrinogens, which host Cs^+ cations by fourfold π-coordination, whereas only two such interactions are actualized in the case of K^+ cations due to their higher propensity to formation of more common K—N bonds (Bonomo *et al.*, 2001). In this way the ninefold coordination of Cs1 comprises one pyrazole-π donor, but even two π-ligands are bonded in the case of eight-coordinate Cs2. These environments are completed with two pyrazole-N [Cs—N = 3.132 (5)–3.392 (6) Å; median 3.26 Å]; nitro- and aqua-O atoms [Cs—O 3.064 (5)–3.754 (7) Å; median 3.17 Å] at the distances approaching the sums of corresponding ionic radii (Cs—N = 3.20; Cs—O = 3.12 Å; Shannon, 1976). The average bond length of eight-coordinate Cs with O-ligands is also in agreement (3.245 Å; Leclaire, 2008). The distorted coordination polyhedra of the Cs^+ ions are nearly intermediate between several idealized geometries. The attribution of these configurations as spherical-relaxed capped cube [Cs1, CN = 9] and triangular dodecahedron [Cs2, CN = 8] is essentially nominal, while considering the best shape measure values of 7.035 and 10.076, respectively, and κ^2-pyrazolate as only one vertex of the polyhedron for Cs2 (Ruiz-Martínez *et al.*, 2008). The relatively poor shape fits are in line with the distortions imposed by the combination of small κ^2-NO_2 and large η^5-pyrazolate ligands.

Every local Cs-pyrazolate-π geometry features the metal ions situated almost exactly above the ring centroids, at the distances of 3.389 (3)–3.587 (3) Å (Table 4), and only slightly shifted from the centroid normal positions toward the ring-N atoms with the slippage angles of 7.5 (3)–20.1 (4)°. There are no precedents of Cs—π-pyrazolate bonding for direct comparison. Similar patterns within a pyrrolate (Heldt & Behrens, 2005; Bonomo *et al.*, 2001) and imidazolate series (Tadokoro *et al.*, 2001) suggest much stronger interactions with the Cs—π (centroid) distances as short as 3.069 Å. Nevertheless, the bonding in **3** may be regarded as very unusual and salient. The second interesting feature, which is unprecedented for nitropyrazolates, is double π-coordination. Unlike the finite arrangement of Cs1—π(ring *A*), the translation-related rings *B* and Cs2 ions sustain an infinite sandwich pattern. These Cs—π bonds are slightly weaker and less directional, in particular due to the elongation of Cs—C separations, up to 3.816 (6)–4.111 (5) Å. One can find that even the electron-depleted nitropyrazolate ligands retain the prominent ability for π-coordination and they are susceptible to interactions with the cations at both axial sides of the ring simultaneously. This kind of weakened bonding may be more selective for the softer Lewis acid Cs^+, unlike stronger metal–π interactions with electron rich pyrazolates (Cortés-Llamas *et al.*, 2006).

The geometry of the organic dianions is consistent with the data for neutral 3,3′-dinitro-4,4′-bipyrazole (Domasevitch *et al.*, 2019). Their common feature consists in a twisted conformation of the molecular framework with two pyrazole rings rotated by 44.96 (7)–48.47 (15)°, while a slightly larger dihedral angle in the case of **3** [57.2 (2)°] is beneficial for specific bonding to Cs ions, which reside at the π-cloud of one ring and coordinate the nitro-O atom from the other ring (Fig. 3). Bond lengths within the pyrazole cores are also very similar to the neutral molecule and its monofunctional prototype 3-nitropyrazole (Foces-Foces *et al.*, 1997). The most salient changes are associated rather with the angles at the ring N^1- (C1—N1—N2 and C4—N4—N5) and N^2-atoms (N1—N2—C3 and N4—N5—C6), which upon ionization become much closer in magnitude, namely 108.2 (4)–108.9 (4)° and 105.70 (17)–106.3 (4)°, respectively, *versus* the more significantly differentiated values of 113.52 (9) and 103.31 (9)° observed for the neutral molecule (Domasevitch *et al.*, 2019). These ring angles are known as good signs for the protolytic state of 3,5-disubstituted pyrazoles in crystal structures since either pyrazolate or pyrazolium ions feature their exact equalization (Domasevitch, 2008). In the case of 3-nitropyrazolates the latter criteria may be less reliable as the anionic forms in **1**–**3** retain a perceptible difference of these parameters.

3. Supramolecular features

The extended structures of compounds **1** and **2** are very similar, both with regard to coordination and the resulting supramolecular arrangements. The intrinsic significance of M—N coordination is reflected by the assembly of readily distinguishable tight metal-organic layers, which are further interconnected in a third dimension with a set of weaker M–nitro-O interactions (Figs. 4 and 5). The primary M-pyrazolato connectivities themselves are only one-periodic and they are very simple. Double chains of metal ions adopt ladder-like motifs with the rung spacings 3.768 Å (**1**) and 3.967 Å (**2**) corresponding to the *b* and to the *a* parameters of the respective unit cells. Every section of these ladders accommodate two μ_4-κ^1:κ^1:κ^1:κ^1 pyrazolate anions, above and below the M_4 plane. This coordination mode is known, for example,

for $[Na_8(tBu_2pz)_6O]$ [tBu_2pz is 3,5-di(*t*-butyl)pyrazolate; Beaini *et al.*, 2007], but it is relatively rare for alkali metal pyrazolates (Deacon *et al.*, 2000; Halcrow, 2009). A very subtle difference between these subconnectivities concerns the mutual orientation of the nitro groups, which are co-aligned in **2** (Fig. 5), but point in opposite directions in **1** (Fig. 4).

Since the organic anions are bifunctional, they serve as connectors between the adjacent coordination ladders that result in the generation of the layers, which are parallel to the *ab* plane in **1** and the *ac* plane in **2**. Accordingly, the interlayer spacings correspond to $\frac{1}{2}c$ = 6.99 Å (**1**) or $\frac{1}{2}b$ = 7.10 Å (**2**) parameters of the unit cells. These separations are nearly identical and therefore one can suppose that the larger Rb^+ ions support stronger interlayer bonding. The latter concerns multiple *M*—nitro-O interactions and, indeed, they are more extensive in the case of *M* = Rb. In **1**, the coordination of NO_2 is μ_3-κ^2:κ^1:κ^1 and three out of four K—O bonds are generated between the layers as the links for two adjacent K ions along the ladder. This chelate-bridging mode is frequently observed for alkali metal ions and nitro ligands (Mendoza-Báez *et al.*, 2024). However, one of the bonds per nitro group is significantly elongated [*e.g.* K1—O2^{v} = 3.418 (3) Å and K2—O3^{vi} = 3.153 (2) Å; symmetry codes: (v) $-x+\frac{1}{2}, y-1, z$ - 1/2; (vi) $-x+\frac{1}{2}, y+1, z+\frac{1}{2}$] and they may be regarded as secondary weak dipole–dipole interactions. In **2**, the coordination modes are μ_3-κ^2:κ^1:κ^1 (N3/O1/O2) and μ_3-κ^2:κ^2:κ^1 (N6/O3/O4). The latter mode generates one additional M—O bond, as may be compared with the K analogue. In addition, even the most distal contact with the larger Rb ion [Rb2—O2^{v} = 3.370 (5) Å; symmetry code (v): $-x+\frac{1}{2}, y-\frac{1}{2}, -z+\frac{1}{2}$] is shorter than the similar long bond for **1**.

The extended structure of **3** is completely different being dominated by cation–π bonding. We identify coordination layers lying parallel to the *bc* plane, in which the infinite Cs2–π(ring *B*)–Cs2–π(ring *B*) stacks along the *b*-axis direction

Table 5
Geometry of hydrogen bonding (Å, °) for **1**–**3**.

Compound	*D*—H···*A*	*D*—H	H···*A*	*D*···*A*	*D*—H···*A*
1	C4—H4···O3^{x}	0.94	2.62	3.352 (4)	135
2	C4—H4···O2^{viii}	0.95	2.68	3.506 (6)	146
3	O1*w*—H1*w*···N1^{vii}	0.85	2.01	2.855 (7)	171
	O1*w*—H2*w*···N5^{vi}	0.85	2.50	3.334 (9)	168
	C1—H1···O2^{iii}	0.94	2.83	3.508 (10)	130
	C4—H4···O1^{viii}	0.94	2.62	3.547 (9)	168

Symmetry codes for **1**: (*x*) $-x, -y, z+\frac{1}{2}$; for **2**: (viii) $x-1, y, z$; for **3**: (iii) $x, y-1, z$; (vi) $-x, y+\frac{1}{2}, -z+1$; (vii) $-x+1, y+\frac{1}{2}, -z+2$; (viii) $-x, y-\frac{1}{2}, -z+2$.

are interlinked through the Cs1–π(ring *A*) fragments with ring *A* coordinated to Cs2 in a κ^2-fashion (Fig. 6), when two bond distances appear to be comparable in length [Cs2—N1^{v} = 3.251 (4) and Cs2—N2^{v} = 3.490 (4) Å; symmetry code: (v) *x*, *y*, *z* − 1.] However, attribution of the layers is only nominal, unlike **1** and **2**. There is no leading significance of *M*—N over *M*—O bonding and both kinds of conventional ionic interactions are equally important either for intra- or interlayer connection. In this way, the above stacks afford two different motifs of mutual interactions (Fig. 7), by the reciprocal bonding of Cs ions and pyrazolate-N atoms between the layers [Cs—N4^{iv} = 3.132 (5) Å; symmetry code: (iv) $x+1, y, z$)], while similar reciprocal coordination of pseudochelate nitro groups-O3/O4 unite the stacks within the layer [Cs2—O = 3.350 (5) and 3.502 (6) Å]. In addition, the water molecules sit above and below the layers and they bridge the Cs1 and Cs2 ions with the comparable relatively long distances Cs—O = 3.215 (6) and 3.496 (7) Å and adopt an even more distal contact to the adjacent layer [Cs1—O1*w*^{i} = 3.754 (7) Å; symmetry code (i) $-x+1, y-\frac{1}{2}, -z+2$]. They are also important as conventional hydrogen-bond donors to the most nucleophilic pyrazolate-N sites (Table 5), with the strongest bonds observed between the layers [O1*w*···N1^{vii} = 2.855 (7) Å, with a nearly linear angle at the H atom of 171°;

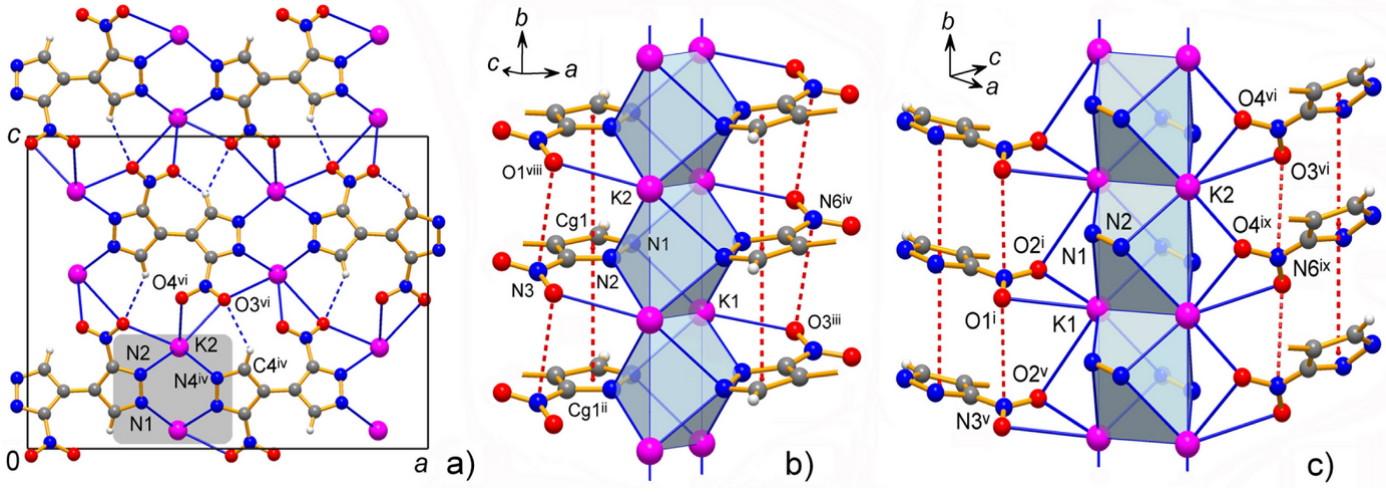

Figure 4
(*a*) Coordination layers in **1** viewed in the projection on the *ac* plane, with the grey box indicating primary K-pyrazolate chains, which are orthogonal to the drawing plane. (*b*) Side-view of the latter showing bridging function of pyrazolates and (*c*) bridging function of NO_2 groups, with the particularly long K1···O2^{v} contacts. Red dotted lines indicate weak stacking interactions. [Symmetry codes: (i) $-x+\frac{1}{2}, y, z-\frac{1}{2}$; (ii) $x, y-1, z$; (iii) $x+\frac{1}{2}, -y-1, z$; (iv) $x+\frac{1}{2}, -y, z$; (v) $-x+\frac{1}{2}, y-1, z-\frac{1}{2}$; (vi) $-x+\frac{1}{2}, y+1, z+\frac{1}{2}$; (viii) $x, y+1, z$; (ix) $-x+\frac{1}{2}, y, z+\frac{1}{2}$.]

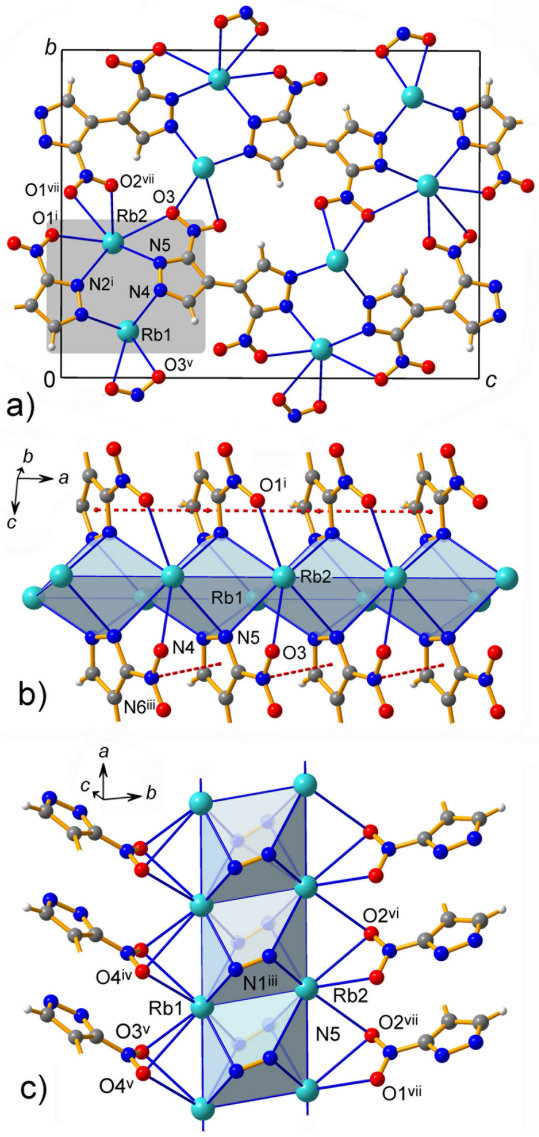

Figure 5
(*a*) Coordination layers in **2** viewed in the projection on the *bc* plane. The grey box indicates Rb–pyrazolate chains, which are orthogonal to the drawing plane. (*b*), (*c*) Two side views of the Rb–pyrazolate ladders along the *a*-axis direction showing the bridging function of the pyrazolates and NO_2 groups. Red dotted lines indicate weak stacking interactions. [Symmetry codes: (i) $x-\frac{1}{2}, -y+\frac{1}{2}, z-\frac{1}{2}$; (iii) $x+\frac{1}{2}, -y+\frac{1}{2}, z-\frac{1}{2}$; (iv) $-x+\frac{3}{2}, y-\frac{1}{2}, -z+\frac{1}{2}$; (v) $-x+\frac{1}{2}, y-\frac{1}{2}, -z+\frac{1}{2}$; (vi) $-x+\frac{3}{2}, y+\frac{1}{2}, -z+\frac{1}{2}$; (vii) $-x+\frac{1}{2}, y+\frac{1}{2}, -z+\frac{1}{2}$.]

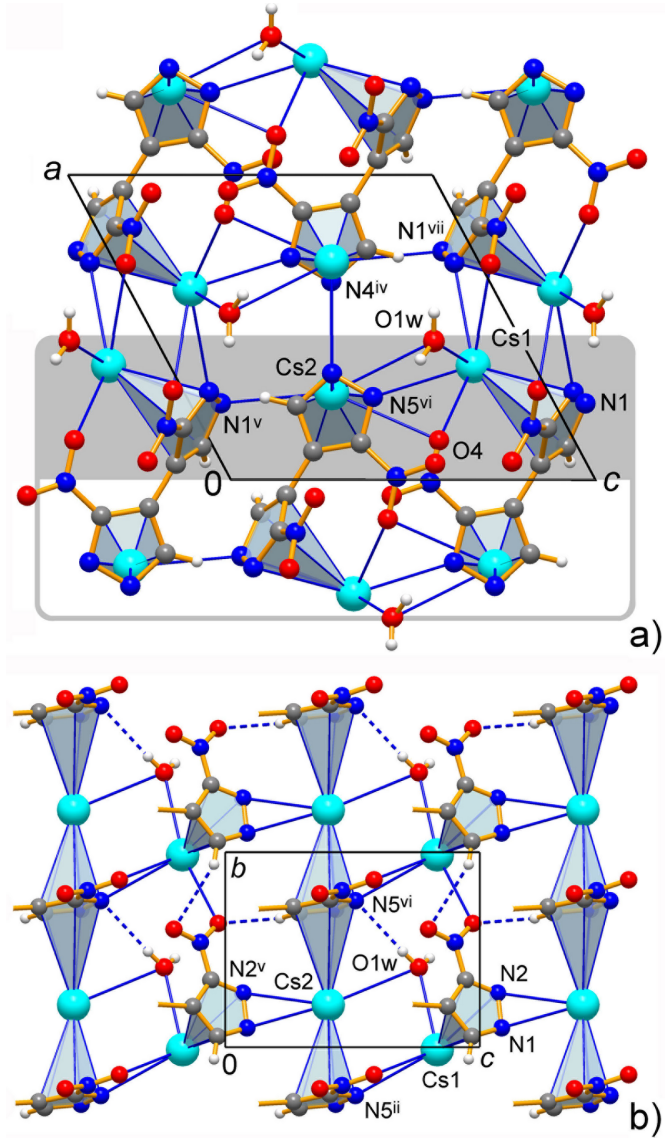

Figure 6
(*a*) Projection of the structure of **3** on the *ac* plane. The grey box indicates the nominal coordination layer, which is orthogonal to the drawing plane, and the grey-shaded area identifies the half-layer, which is further described (*b*) in its projection on the *bc* plane. Note the co-existence of the finite [Cs1] and chain-like [Cs2] π-coordination patterns. [Symmetry codes: (ii) $-x, y-\frac{1}{2}, -z+1$; (v) $x, y, z-1$; (vi) $-x, y+\frac{1}{2}, -z+1$; (vii) $-x+1, y+\frac{1}{2}, -z+2$.]

symmetry code: (vii) $-x+1, y+\frac{1}{2}, -z+2$]. The accessibility of pyrazolate-N acceptors for the hydrogen bonding is conditioned by the preferential Cs–π coordination over formation of Cs—N bonds. Therefore, the incorporation of water molecules in **3**, in contrast to the formation of anhydrates **1** and **2**, may be regarded as a response to the needs for appropriate structural pairing of hard Lewis basic N atoms.

In addition to the main structure-defining Coulombic forces, ion–dipole bonding and conventional hydrogen bonding in **3**, the structures also reveal a variety of weak secondary interactions, which complement the coordination patterns. They include weak C—H···O hydrogen bonding with polarized pyrazole CH donors and nitro-O acceptors (Table 5) and different stacking interactions with the formation of either homo- (pyrazole/pyrazole, nitro/nitro) or heterofunctional pairs (pyrazole/nitro) (Table 6). The significance of weak hydrogen bonds is rather minor. All of them are found within the topological layers and they accompany the configurations imposed by coordination, with typical C···O separations in the range of 3.352 (4)–3.547 (9) Å (Desiraju & Steiner, 1999). The stacking of the rings is irrelevant for **3** since the axial positions at the pyrazole rings serve for the accommodation of Cs ions. Such interactions contribute to the suite of weak bonding interactions in the case of **1** and **2** between the coordination layers. In every case the π–π contacts are very

Table 6
Geometry of stacking interactions (Å, °) for **1**–**3**.

*Cg*1···*Cg*2 is the distance between the centroids of Group 1 and Group 2; *Cg*1···Plane is the distance from the Group 1 centroid to the mean plane of Group 2 or the distance of an O-donor to the mean plane of a nitro group; sa is the slippage angle *i.e.* the angle of the *Cg*1···*Cg*2 axis to the plane of Group 2 or the angle of the O···N axis to the plane of the nitro group for the NO_2/NO_2 patterns.

Compound	Type	Group 1	Group 2	Shortest contact	*Cg*1···*Cg*2	*Cg*1···Plane	sa
1	Pyrazole/Pyrazole	(N1/N2/C1–3)	(N1/N2/C1–3)^{ii}	3.492 (3)	3.768 (3)	3.479 (4)	22.6 (4)
	Pyrazole/Pyrazole	(N4/N5/C4–6)	(N4/N5/C4–6)^{ii}	3.456 (3)	3.768 (3)	3.470 (4)	22.9 (4)
	NO_2/NO_2	(C3/N3/O1/O2)	(C3/N3/O1/O2)^{ii}	3.238 (3)	–	3.104 (3)	16.5 (5)
	NO_2/NO_2	(C6/N6/O3/O4)	(C6/N6/O3/O4)^{ii}	3.298 (3)	–	3.176 (4)	15.6 (6)
2	Pyrazole/Pyrazole	(N1/N2/C1–3)	(N1/N2/C1–3)^{ii}	3.707 (7)	3.967 (6)	3.689 (7)	21.6 (7)
	Pyrazole/NO_2	(N4/N5/C4–6)	(C6/N6/O3/O4)^{viii}	3.375 (6)	3.402 (6)	3.374 (7)	7.4 (8)
	NO_2/NO_2	(C3/N3/O1/O2)	(C3/N3/O1/O2)^{ii}	3.354 (8)	–	3.150 (8)	20.1 (8)
3	NO_2/NO_2	(C6/N6/O3/O4)	(C6/N6/O3/O4)^{vi}	3.142 (8)	–	2.871 (9)	24.0 (8)

Symmetry codes for **1**: (ii) $x, y-1, z$; for **2**:(ii) $x+1, y, z$; (viii) $x-1, y, z$; for **3**: (vi) $-x, y+\frac{1}{2}, -z+1$.

distal, with the intercentroid distances up to 3.967 (7) Å and relatively large slippage angles (Table 6). The *B* rings in **2** do not support overlap at all, but produce the relatively close stacks of pyrazole and NO_2 groups with the nitro-N atoms residing exactly above the ring centroids at 3.402 (6) Å. Yet another kind of weak bond is the lone pair–π-hole interaction (Bauzá *et al.*, 2017), which is equally relevant for each of the three structures, in the form of mutual NO_2/NO_2 stacking. Such interactions themselves could be superior in energetics to the common weak hydrogen bonds and they are one of the dominant factors for the crystal structures of polynitro species (Domasevitch *et al.*, 2020). However, in the present case these interactions are weak or very weak, as indicated by the corresponding N···O contacts at 3.142 (8)–3.354 (8) Å (Table 6), which are longer than the sum of van der Waals radii (3.07 Å).

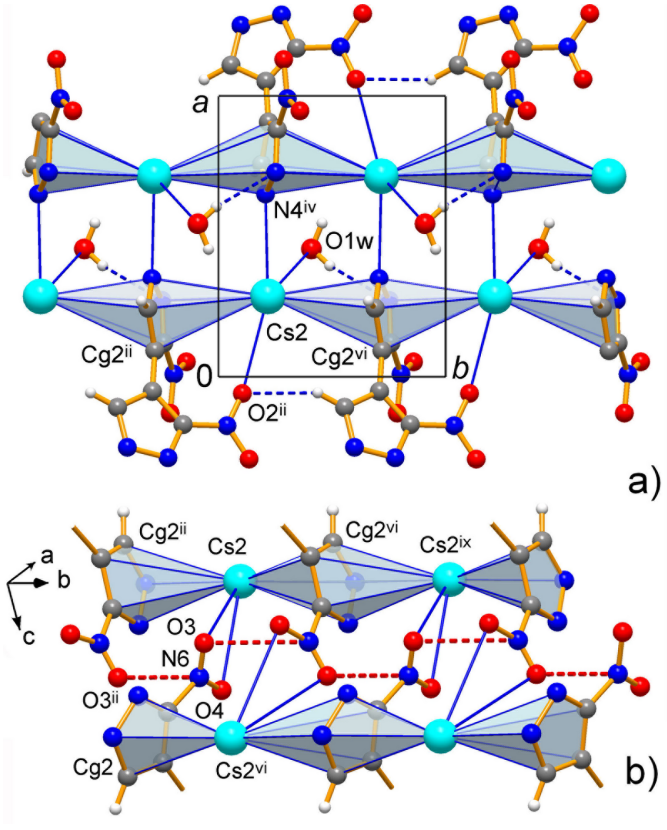

Figure 7
Two fragments of the structure of **3**, which depict one-dimensional Cs–π chains along the *b*-axis direction and their aggregation through reciprocal Cs—N bonds (*a*) and Cs—O bonds (*b*) leading to the generation of the infinite NO_2/NO_2 stack. [Symmetry codes: (ii) $-x, y-\frac{1}{2}, -z+1$; (iv) $x+1, y, z$; (vi) $-x, y+\frac{1}{2}, -z+1$; (ix) $x, y+1, z$.]

4. Database survey

A search of the Cambridge Structural Database (CSD version 5.43, update of November 2022; Groom *et al.*, 2016) reveals no late alkali metal (K, Rb, Cs) mononitropyrazolates, while a series of the salts with different dinitropyrazolate anions accounts for thirteen hits. Unless the nucleophilic N sites are blocked by strong N bonding, most of them display multiple pyrazolate-N coordinations, which is reminiscent of that observed for **1** and **2**. In particular, a rare mode μ_4-κ^1:κ^1:κ^1:κ^1 was found for (μ-3,5-dinitropyrazolid-4-olato)dicaesium (CSD refcode BEGXUK; Dong *et al.*, 2022), while its Rb analogue (BEGYAR; Dong *et al.*, 2022), (μ-3,4-dinitropyrazolato)caesium (EDOTOK; Cao *et al.*, 2022) and (μ-3,5-dinitropyrazolato)potassium (GIMPEA; Bölter *et al.*, 2018) provide tetradentate bridges of the type μ_3-κ^2:κ^1:κ^1. There are no unambiguous examples for the metal–π-nitropyrazolate coordination at all, which is not surprising for such electron-depleted systems. However, some cases revealed the metal ions situated nearly above the N atoms, at one of the axial sides of the ring. This may presumably be regarded as a very distal weak cation–π interaction, which is accompanied with large slippage angles due to the significant shift of M^+ toward more negatively polarized atoms. In this way, in GIMPEA the K^+ to ring centroid distance is 3.41 Å, which is close to the parameters of **3** for the much larger Cs^+ ion. A similar Rb···π contact of 3.40 Å is present in BEGYAR. Caesium 4-(pyrazol-4-yl)-3,5-dinitropyrazolate monohydrate (FUFBIU; Gospodinov *et al.*, 2020) exhibits no Cs···π interactions to pyrazolate, but instead a very long such contact (3.67 Å) is found for the neutral pyrazol-4-yl ring. This feature disappears in the structure of the more electron-deficient trinitro analogue (FUFCIV; Gospodinov *et al.*, 2020).

Table 7
Experimental details.

	1	2	3
Crystal data			
Chemical formula	$[K_2(C_6H_2N_6O_4)]$	$[Rb_2(C_6H_2N_6O_4)]$	$[Cs_2(C_6H_2N_6O_4)]\cdot H_2O$
M_r	300.34	393.08	505.97
Crystal system, space group	Orthorhombic, $Pca2_1$	Monoclinic, $P2_1/n$	Monoclinic, $P2_1$
Temperature (K)	213	173	213
a, b, c (Å)	18.7276 (19), 3.7683 (3), 13.9808 (13)	3.9669 (2), 14.2020 (4), 18.6685 (6)	9.7388 (7), 6.9551 (3), 10.2950 (7)
α, β, γ (°)	90, 90, 90	90, 95.776 (3), 90	90, 118.152 (8), 90
V (Å^3)	986.64 (16)	1046.40 (7)	614.83 (8)
Z	4	4	2
Radiation type	Mo $K\alpha$	Cu $K\alpha$	Mo $K\alpha$
μ (mm^{-1})	0.98	12.38	5.96
Crystal size (mm)	0.22 × 0.21 × 0.18	0.05 × 0.03 × 0.03	0.20 × 0.17 × 0.14
Data collection			
Diffractometer	Stoe Image plate diffraction system-2T	Stoe Stadivari	Stoe Image plate diffraction system-2T
Absorption correction	Numerical [*X-RED* (Stoe & Cie, 2001) and *X-SHAPE* (Stoe & Cie, 1999)]	Multi-scan (Stoe *LANA*; Kozis-kova *et al.*, 2016)	Numerical [*X-RED* (Stoe & Cie, 2001) and *X-SHAPE* (Stoe & Cie, 1999)]
T_{min}, T_{max}	0.854, 0.871	0.469, 0.661	0.218, 0.245
No. of measured, independent and observed [$I > 2\sigma(I)$] reflections	6480, 2285, 1849	10655, 2234, 2156	4971, 2554, 2376
R_{int}	0.022	0.030	0.020
(sin $\theta/\lambda)_{max}$ (Å^{-1})	0.660	0.638	0.641
Refinement			
$R[F^2 > 2\sigma(F^2)]$, $wR(F^2)$, S	0.021, 0.048, 0.91	0.048, 0.148, 1.14	0.020, 0.045, 0.99
No. of reflections	2285	2234	2554
No. of parameters	164	164	173
No. of restraints	1	0	1
H-atom treatment	H-atom parameters constrained	H-atom parameters constrained	H-atom parameters constrained
$\Delta\rho_{max}$, $\Delta\rho_{min}$ (e Å^{-3})	0.22, −0.19	0.86, −0.73	0.93, −1.17
Absolute structure	Refined as an inversion twin	–	Refined as an inversion twin
Absolute structure parameter	0.41 (4)	–	0.44 (3)

Computer programs: *IPDS Software* (Stoe & Cie, 2000), *X-AREA 1.76* (Stoe & Cie, 2016), *SHELXS97* (Sheldrick, 2008), *SHELXL2019/3* (Sheldrick, 2015), *DIAMOND 3.0* (Brandenburg, 1999) and *WinGX 1.70.01* (Farrugia, 2012).

5. Synthesis and crystallization

The ligand 3,3′-dinitro-4,4′-bipyrazole was prepared in 79% yield by nitration of 4,4′-bipyrazole in phosphoric acid (Domasevitch *et al.*, 2019). This synthesis is not routine since the common nitration of the substrate in mixed acids proceeds through attack on a deactivated pyrazolium cation (Austin *et al.*, 1965), but the mononitrated ring readily undergoes second substitution as more reactive free base. This results in the apparent paradox of dinitration at the same ring with the production of isomeric 3,5-dinitro-4,4′-bipyrazole. Therefore the utilization of less acidic H_3PO_4 is a key pre-requisite for the success of preparation.

To prepare the alkali metal salts, 34 mg (0.15 mmol) of 3,3′-dinitro-4,4′-bipyrazole were dissolved in 3 ml of 20% aqueous solution of alkali metal (K, Rb or Cs) hydroxide under stirring and heating to 333–343 K. The resulting clear dark-red solution was left overnight, after which the crystalline deposit of orange–red bipyrazolate salt (yields 70–80%) was filtered and washed with 1–2 ml of 2-propanol.

Analysis (%) calculated for (**1**), $C_6H_2K_2N_6O_4$: C 23.99, H 0.67, N 27.99; found: C 23.67, H 0.81, N 27.70. Analysis (%) calculated for (**2**), $C_6H_2N_6O_4Rb_2$: C 18.33, H 0.51, N 21.39; found: C 18.27, H 0.68, N 21.08. Analysis (%) calculated for (**3**), $C_6H_4Cs_2N_6O_5$: C 14.24, H 0.80, N 16.61; found: C 14.02, H 0.88, N 16.38.

6. Refinement

Crystal data, data collection and structure refinement details are summarized in Table 7. Structures **1** and **3** were refined as inversion twins with partial contribution factors 0.587/0.413 and 0.563/0.437, respectively. The water H atoms in **3** were located and then restrained with O—H = 0.85 Å and U_{iso} = 1.5U_{eq} (carrier O-atom), whereas all C-bound hydrogen atoms were constrained geometrically and refined as riding with U_{iso}(H) = 1.2U_{eq}(carrier C-atom).

Funding information

This work was supported by the Ministry of Education and Science of Ukraine (project No. 25BF037–02).

References

Austin, M. W., Blackborow, J. R., Ridd, J. H. & Smith, B. V. (1965). *J. Chem. Soc.* pp. 1051–1057.

Bauzá, A., Sharko, A. V., Senchyk, G. A., Rusanov, E. B., Frontera, A. & Domasevitch, K. V. (2017). *CrystEngComm* **19**, 1933–1937.
Beaini, S., Deacon, G. B., Erven, A. P., Junk, P. C. & Turner, D. R. (2007). *Chem. Asian J.* **2**, 539–550.
Blanco, F., Alkorta, I. & Elguero, J. (2008). *J. Phys. Chem. A* **112**, 7682–7688.
Bölter, M. F., Harter, A., Klapötke, T. M. & Stierstorfer, J. (2018). *ChemPlusChem* **83**, 804–811.
Bonomo, L., Solari, E., Scopelliti, R. & Floriani, C. (2001). *Chem. Eur. J.* **7**, 1322–1332.
Brandenburg, K. (1999). *DIAMOND*. Release 2.1e. Crystal Impact GbR, Bonn, Germany.
Cao, W., Wang, T., Mei, H., Dong, W., Tariq, Q., Yin, L., Li, Z. & Zhang, J. (2022). *ACS Appl. Mater. Interfaces* **14**, 32084–32095.
Cortés-Llamas, S.-A., Hernández-Lamoneda, R., Velázquez-Carmona, M.-A., Muñoz-Hernández, V.-A. & Toscano, R. A. (2006). *Inorg. Chem.* **45**, 286–294.
Deacon, G. B., Delbridge, E. E., Forsyth, C. M., Skelton, B. W. & White, A. H. (2000). *J. Chem. Soc. Dalton Trans.* pp. 745–751.
Desiraju, G. R. & Steiner, T. (1999). *The Weak Hydrogen Bond in Structural Chemistry and Biology*. Oxford University Press.
Domasevitch, K. V. (2008). *Acta Cryst.* C**64**, o326–o329.
Domasevitch, K. V., Gospodinov, I., Krautscheid, H., Klapötke, T. M. & Stierstorfer, J. (2019). *New J. Chem.* **43**, 1305–1312.
Domasevitch, K. V., Senchyk, G. A. & Krautscheid, H. (2020). *Acta Cryst.* C**76**, 598–604.
Dong, W.-S., Wang, X., Zhang, C., Zhang, L., Hu, Y., Cao, W., Wu, X., Wang, T. & Zhang, J.-G. (2022). *Cryst. Growth Des.* **22**, 5449–5458.
Dougherty, D. A. (2025). *Chem. Rev.* **125**, 2793–2808.
Fabbrizzi, L. (2020). *ChemTexts* **6**: 10. https:/doi.org/10.1007/s40828-020-0107-2
Farrugia, L. J. (2012). *J. Appl. Cryst.* **45**, 849–854.
Foces-Foces, C., Llamas-Saiz, A. L., Menendez, M., Jagerovic, N. & Elguero, J. (1997). *J. Phys. Org. Chem.* **10**, 637–645.
Gospodinov, I., Domasevitch, K. V., Unger, C. C., Klapötke, T. M. & Stierstorfer, J. (2020). *Cryst. Growth Des.* **20**, 755–764.
Groom, C. R., Bruno, I. J., Lightfoot, M. P. & Ward, S. C. (2016). *Acta Cryst.* B**72**, 171–179.
Halcrow, M. A. (2009). *Dalton Trans.*, pp. 2059–2073.
Heldt, I. & Behrens, U. (2005). *Z. Anorg. Allg. Chem.*, **631**, 749–758.
Janssen, J. W. A. M., Kruse, C. C., Koeners, H. J. & Habraken, C. (1973). *J. Heterocycl. Chem.* **10**, 1055–1058.
Koziskova, J., Hahn, F., Richter, J. & Kožišek, J. (2016). *Acta Chim. Slovaca* **9**, 136–140.
Leclaire, A. (2008). *J. Solid State Chem.* **181**, 2338–2345.
Mendoza-Báez, R., Molina-Renteria, A. & Olguín, J. (2024). *CrystEngComm* **26**, 2346–2352.
Pink, M. & Sieler, J. (2007). *Inorg. Chim. Acta* **360**, 1221–1225.
Ruiz-Martínez, A., Casanova, D. & Alvarez, S. (2008). *Chem. Eur. J.* **14**, 1291–1303.
Shannon, R. D. (1976). *Acta Cryst.* A**32**, 751–767.
Sheldrick, G. M. (2008). *Acta Cryst.* A**64**, 112–122.
Sheldrick, G. M. (2015). *Acta Cryst.* C**71**, 3–8.
Stoe & Cie (1999). *X-SHAPE*. Revision 1.06. Stoe & Cie GmbH, Darmstadt, Germany.
Stoe & Cie (2000). *IPDS Software*. Stoe & Cie GmbH, Darmstadt, Germany.
Stoe & Cie (2001). *X-RED*. Version 1.22. Stoe & Cie GmbH, Darmstadt, Germany.
Stoe & Cie (2016). *X-AREA 1.76*. Stoe & Cie GmbH, Darmstadt, Germany.
Tadokoro, M., Shiomi, T., Isobe, K. & Nakasuji, K. (2001). *Inorg. Chem.* **40**, 5476–5478.
Watt, M., Hwang, J., Cormier, K. W. & Lewis, M. (2009). *J. Phys. Chem. A* **113**, 6192–6196.
Woods, J. (2016). *Structural Variations Involving s-block Metal Pyrazolates*. Renée Crown University Honors Thesis Projects - All. 925. https://surface.syr.edu/honors_capstone/925.
Yamada, S. (2020). *Coord. Chem. Rev.* **415**, 213301.

supporting information

Acta Cryst. (2026). E**82**, 683-691 [https://doi.org/10.1107/S2056989026005037]

Dibasic 3,3′-dinitro-4,4′-bipyrazole-1,1′-diides of K, Rb and Cs reveal metal-selective ring–π over ring–N coordination

Kostiantyn V. Domasevitch and Vira V. Ponomarova

Computing details

Poly[[μ-3,3′-dinitro-4,4′-bipyrazole-1,1′-diido]dipotassium] (1)

Crystal data

$[K_2(C_6H_2N_6O_4)]$
M_r = 300.34
Orthorhombic, $Pca2_1$
a = 18.7276 (19) Å
b = 3.7683 (3) Å
c = 13.9808 (13) Å
V = 986.64 (16) Å^3
Z = 4
$F(000)$ = 600
D_x = 2.022 Mg m^{-3}
Mo $K\alpha$ radiation, λ = 0.71073 Å
Cell parameters from 6480 reflections
θ = 2.6–28.0°
μ = 0.98 mm^{-1}
T = 213 K
Prism, red
0.22 × 0.21 × 0.18 mm

Data collection

Stoe Image plate diffraction system-2T diffractometer
Radiation source: fine-focus sealed tube
φ oscillation scans
Absorption correction: numerical [X-RED (Stoe & Cie, 2001) and X-SHAPE (Stoe & Cie, 1999)]
T_{min} = 0.854, T_{max} = 0.871
6480 measured reflections
2285 independent reflections
1849 reflections with $I > 2\sigma(I)$
R_{int} = 0.022
θ_{max} = 28.0°, θ_{min} = 2.6°
h = −24→24
k = −4→4
l = −18→18

Refinement

Refinement on F^2
Least-squares matrix: full
$R[F^2 > 2\sigma(F^2)]$ = 0.021
$wR(F^2)$ = 0.048
S = 0.91
2285 reflections
164 parameters
1 restraint
Primary atom site location: structure-invariant direct methods
Secondary atom site location: difference Fourier map
Hydrogen site location: inferred from neighbouring sites
H-atom parameters constrained
$w = 1/[\sigma^2(F_o^2) + (0.0272P)^2]$ where $P = (F_o^2 + 2F_c^2)/3$
$(\Delta/\sigma)_{max} < 0.001$
$\Delta\rho_{max}$ = 0.22 e Å^{-3}
$\Delta\rho_{min}$ = −0.19 e Å^{-3}
Absolute structure: Refined as an inversion twin
Absolute structure parameter: 0.41 (4)

Special details

Geometry. All esds (except the esd in the dihedral angle between two l.s. planes) are estimated using the full covariance matrix. The cell esds are taken into account individually in the estimation of esds in distances, angles and torsion angles; correlations between esds in cell parameters are only used when they are defined by crystal symmetry. An approximate (isotropic) treatment of cell esds is used for estimating esds involving l.s. planes.

Refinement. Refined as a 2-component inversion twin.

Fractional atomic coordinates and isotropic or equivalent isotropic displacement parameters (Å²)

	x	*y*	*z*	U_{iso}*/U_{eq}
K1	0.37544 (4)	−0.49087 (18)	0.05811 (4)	0.02022 (13)
K2	0.37880 (3)	0.37981 (18)	0.32366 (3)	0.02035 (14)
O1	0.23811 (12)	−0.4115 (7)	0.39913 (17)	0.0331 (6)
O2	0.13683 (12)	−0.1418 (9)	0.38871 (16)	0.0418 (7)
O3	0.00886 (11)	−0.3670 (7)	−0.02285 (16)	0.0301 (5)
O4	0.11495 (11)	−0.1447 (7)	−0.01775 (15)	0.0323 (6)
N1	0.28453 (13)	0.0267 (7)	0.1470 (2)	0.0210 (6)
N2	0.28173 (12)	−0.1085 (8)	0.23656 (18)	0.0186 (5)
N3	0.19516 (12)	−0.2269 (8)	0.35423 (17)	0.0220 (6)
N4	−0.02670 (12)	0.1315 (8)	0.22521 (17)	0.0194 (5)
N5	−0.02718 (13)	−0.0134 (7)	0.1359 (2)	0.0193 (6)
N6	0.05558 (13)	−0.1962 (7)	0.01939 (16)	0.0203 (6)
C1	0.21717 (15)	0.1044 (9)	0.1183 (2)	0.0194 (6)
H1	0.205558	0.199449	0.058094	0.023*
C2	0.16761 (15)	0.0263 (9)	0.1887 (2)	0.0158 (9)
C3	0.21248 (14)	−0.1040 (9)	0.2612 (2)	0.0162 (6)
C4	0.04169 (14)	0.1663 (9)	0.2536 (2)	0.0186 (6)
H4	0.055404	0.256931	0.313491	0.022*
C5	0.08971 (15)	0.0525 (10)	0.18402 (19)	0.0146 (7)
C6	0.04176 (14)	−0.0536 (8)	0.1116 (2)	0.0153 (6)

Atomic displacement parameters (Å²)

	U^{11}	U^{22}	U^{33}	U^{12}	U^{13}	U^{23}
K1	0.0164 (2)	0.0229 (3)	0.0214 (3)	0.0004 (2)	0.0000 (3)	0.0051 (2)
K2	0.0201 (3)	0.0204 (4)	0.0206 (3)	−0.0003 (3)	−0.0016 (3)	−0.0004 (2)
O1	0.0296 (12)	0.0443 (17)	0.0253 (12)	0.0093 (11)	−0.0059 (10)	0.0116 (10)
O2	0.0216 (11)	0.076 (2)	0.0273 (12)	0.0113 (12)	0.0091 (9)	0.0202 (12)
O3	0.0267 (11)	0.0450 (16)	0.0186 (10)	−0.0112 (11)	−0.0024 (9)	−0.0077 (10)
O4	0.0203 (11)	0.0539 (17)	0.0227 (10)	−0.0065 (11)	0.0068 (9)	−0.0112 (10)
N1	0.0146 (12)	0.0240 (19)	0.0244 (15)	−0.0021 (10)	0.0025 (10)	0.0002 (10)
N2	0.0114 (11)	0.0229 (16)	0.0216 (13)	−0.0013 (10)	0.0007 (9)	−0.0007 (11)
N3	0.0181 (12)	0.0302 (17)	0.0178 (11)	−0.0020 (10)	−0.0024 (9)	0.0016 (10)
N4	0.0143 (11)	0.0253 (17)	0.0187 (12)	0.0020 (10)	0.0027 (9)	−0.0019 (12)
N5	0.0154 (11)	0.0219 (18)	0.0207 (14)	0.0001 (9)	−0.0016 (9)	−0.0005 (10)
N6	0.0184 (12)	0.0258 (17)	0.0167 (11)	0.0014 (10)	−0.0012 (9)	0.0016 (10)
C1	0.0173 (14)	0.0224 (18)	0.0186 (14)	−0.0014 (12)	0.0020 (10)	0.0016 (13)
C2	0.0133 (12)	0.015 (2)	0.0191 (18)	−0.0002 (11)	−0.0021 (11)	−0.0022 (10)

C3	0.0139 (13)	0.0183 (17)	0.0163 (15)	−0.0010 (11)	−0.0002 (10)	0.0002 (12)
C4	0.0151 (12)	0.022 (2)	0.0189 (14)	0.0023 (11)	0.0004 (10)	−0.0021 (11)
C5	0.0149 (12)	0.016 (2)	0.0127 (16)	−0.0005 (13)	0.0020 (10)	0.0025 (10)
C6	0.0123 (13)	0.0170 (18)	0.0167 (15)	0.0007 (10)	−0.0004 (10)	0.0009 (11)

Geometric parameters (Å, º)

K1—O2^{i}	2.719 (2)	O3—N6	1.236 (3)
K1—N1^{ii}	2.783 (3)	O4—N6	1.242 (3)
K1—O3^{iii}	2.795 (2)	N1—N2	1.353 (4)
K1—N5^{iii}	2.828 (3)	N1—C1	1.356 (4)
K1—N5^{iv}	2.850 (3)	N2—C3	1.342 (3)
K1—N1	2.871 (3)	N3—C3	1.418 (4)
K1—O1^{i}	3.091 (3)	N4—C4	1.347 (4)
K1—O2^{v}	3.418 (3)	N4—N5	1.362 (4)
K2—O4^{vi}	2.853 (2)	N5—C6	1.344 (4)
K2—N2	2.859 (3)	N6—C6	1.420 (4)
K2—N4^{vii}	2.901 (3)	C1—C2	1.385 (4)
K2—N2^{viii}	2.917 (3)	C1—H1	0.9400
K2—O1^{viii}	2.945 (2)	C2—C3	1.406 (4)
K2—N4^{iv}	2.956 (3)	C2—C5	1.464 (3)
K2—O4^{ix}	2.973 (3)	C4—C5	1.393 (4)
K2—O3^{vi}	3.153 (2)	C4—H4	0.9400
O1—N3	1.235 (3)	C5—C6	1.411 (4)
O2—N3	1.236 (3)		

O2^{i}—K1—N1^{ii}	130.77 (8)	N6—O4—K2^{i}	116.80 (18)
O2^{i}—K1—O3^{iii}	79.37 (7)	K2^{v}—O4—K2^{i}	80.58 (6)
N1^{ii}—K1—O3^{iii}	127.04 (8)	N2—N1—C1	108.6 (2)
O2^{i}—K1—N5^{iii}	135.17 (8)	N2—N1—K1^{viii}	133.1 (2)
N1^{ii}—K1—N5^{iii}	77.95 (8)	C1—N1—K1^{viii}	107.2 (2)
O3^{iii}—K1—N5^{iii}	56.82 (7)	N2—N1—K1	99.67 (19)
O2^{i}—K1—N5^{iv}	93.68 (8)	C1—N1—K1	124.8 (2)
N1^{ii}—K1—N5^{iv}	131.04 (8)	K1^{viii}—N1—K1	83.56 (7)
O3^{iii}—K1—N5^{iv}	73.16 (8)	C3—N2—N1	105.7 (2)
N5^{iii}—K1—N5^{iv}	83.16 (7)	C3—N2—K2	119.8 (2)
O2^{i}—K1—N1	89.90 (9)	N1—N2—K2	97.32 (19)
N1^{ii}—K1—N1	83.56 (7)	C3—N2—K2^{ii}	120.2 (2)
O3^{iii}—K1—N1	146.67 (8)	N1—N2—K2^{ii}	127.67 (18)
N5^{iii}—K1—N1	131.64 (7)	K2—N2—K2^{ii}	81.45 (7)
N5^{iv}—K1—N1	76.19 (7)	O1—N3—O2	121.6 (3)
O2^{i}—K1—O1^{i}	42.99 (6)	O1—N3—C3	120.1 (2)
N1^{ii}—K1—O1^{i}	87.90 (7)	O2—N3—C3	118.4 (3)
O3^{iii}—K1—O1^{i}	110.02 (8)	O1—N3—K1^{ix}	69.62 (16)
N5^{iii}—K1—O1^{i}	141.65 (8)	O2—N3—K1^{ix}	52.17 (15)
N5^{iv}—K1—O1^{i}	130.57 (7)	C3—N3—K1^{ix}	169.57 (18)
N1—K1—O1^{i}	80.64 (8)	C4—N4—N5	108.4 (2)
O2^{i}—K1—O2^{v}	74.80 (6)	C4—N4—K2^{xi}	112.22 (19)

N1^{ii}—K1—O2^{v}	78.43 (7)	N5—N4—K2^{xi}	133.24 (19)
O3^{iii}—K1—O2^{v}	69.01 (7)	C4—N4—K2^{xii}	119.7 (2)
N5^{iii}—K1—O2^{v}	80.56 (7)	N5—N4—K2^{xii}	99.29 (18)
N5^{iv}—K1—O2^{v}	141.84 (7)	K2^{xi}—N4—K2^{xii}	80.08 (6)
N1—K1—O2^{v}	138.37 (7)	C4—N4—K1^{xii}	134.8 (2)
O1^{i}—K1—O2^{v}	61.63 (7)	N5—N4—K1^{xii}	60.45 (15)
O4^{vi}—K2—N2	139.58 (7)	K2^{xi}—N4—K1^{xii}	74.55 (6)
O4^{vi}—K2—N4^{vii}	86.85 (7)	K2^{xii}—N4—K1^{xii}	105.52 (7)
N2—K2—N4^{vii}	126.46 (8)	C6—N5—N4	105.7 (2)
O4^{vi}—K2—N2^{viii}	86.26 (7)	C6—N5—K1^{x}	116.6 (2)
N2—K2—N2^{viii}	81.45 (7)	N4—N5—K1^{x}	128.42 (19)
N4^{vii}—K2—N2^{viii}	76.26 (7)	C6—N5—K1^{xii}	126.4 (2)
O4^{vi}—K2—O1^{viii}	65.83 (7)	N4—N5—K1^{xii}	94.98 (18)
N2—K2—O1^{viii}	75.85 (7)	K1^{x}—N5—K1^{xii}	83.16 (7)
N4^{vii}—K2—O1^{viii}	123.10 (8)	C6—N5—K2^{xii}	129.7 (2)
N2^{viii}—K2—O1^{viii}	54.23 (7)	N4—N5—K2^{xii}	57.76 (15)
O4^{vi}—K2—N4^{iv}	138.30 (7)	K1^{x}—N5—K2^{xii}	72.49 (6)
N2—K2—N4^{iv}	76.28 (7)	K1^{xii}—N5—K2^{xii}	103.34 (8)
N4^{vii}—K2—N4^{iv}	80.08 (6)	O3—N6—O4	121.0 (2)
N2^{viii}—K2—N4^{iv}	127.57 (7)	O3—N6—C6	120.1 (2)
O1^{viii}—K2—N4^{iv}	151.21 (8)	O4—N6—C6	118.9 (2)
O4^{vi}—K2—O4^{ix}	80.58 (6)	O3—N6—K2^{v}	68.08 (15)
N2—K2—O4^{ix}	85.11 (7)	O4—N6—K2^{v}	54.09 (14)
N4^{vii}—K2—O4^{ix}	138.75 (7)	C6—N6—K2^{v}	167.03 (18)
N2^{viii}—K2—O4^{ix}	140.86 (7)	N1—C1—C2	111.6 (3)
O1^{viii}—K2—O4^{ix}	86.88 (6)	N1—C1—H1	124.2
N4^{iv}—K2—O4^{ix}	83.71 (7)	C2—C1—H1	124.2
O4^{vi}—K2—O3^{vi}	41.73 (6)	K1^{viii}—C1—H1	79.1
N2—K2—O3^{vi}	155.36 (7)	C1—C2—C3	100.7 (2)
N4^{vii}—K2—O3^{vi}	73.96 (7)	C1—C2—C5	128.5 (2)
N2^{viii}—K2—O3^{vi}	120.00 (7)	C3—C2—C5	130.7 (3)
O1^{viii}—K2—O3^{vi}	105.80 (7)	N2—C3—C2	113.4 (3)
N4^{iv}—K2—O3^{vi}	96.58 (6)	N2—C3—N3	116.9 (3)
O4^{ix}—K2—O3^{vi}	70.57 (6)	C2—C3—N3	129.7 (2)
N3—O1—K2^{ii}	123.44 (18)	N4—C4—C5	112.2 (3)
N3—O1—K1^{ix}	88.39 (16)	N4—C4—H4	123.9
K2^{ii}—O1—K1^{ix}	147.93 (8)	C5—C4—H4	123.9
N3—O2—K1^{ix}	106.79 (19)	C4—C5—C6	100.2 (2)
N3—O2—K1^{vi}	121.0 (2)	C4—C5—C2	129.3 (2)
K1^{ix}—O2—K1^{vi}	74.80 (6)	C6—C5—C2	130.3 (3)
N6—O3—K1^{x}	122.62 (17)	N5—C6—C5	113.4 (3)
N6—O3—K2^{v}	90.59 (16)	N5—C6—N6	116.6 (3)
K1^{x}—O3—K2^{v}	144.50 (9)	C5—C6—N6	130.0 (3)
N6—O4—K2^{v}	105.26 (17)		

C1—N1—N2—C3	−1.1 (4)	K1^{viii}—C1—C2—C3	−49.2 (5)
K1^{viii}—N1—N2—C3	136.8 (2)	N1—C1—C2—C5	−176.2 (4)
K1—N1—N2—C3	−133.0 (2)	K1^{viii}—C1—C2—C5	134.4 (4)

C1—N1—N2—K2	−124.9 (2)	N1—N2—C3—C2	1.2 (4)
K1^{viii}—N1—N2—K2	13.0 (3)	K2—N2—C3—C2	109.5 (3)
K1—N1—N2—K2	103.18 (11)	K2^{ii}—N2—C3—C2	−152.7 (2)
C1—N1—N2—K2^{ii}	150.3 (2)	N1—N2—C3—N3	−178.7 (3)
K1^{viii}—N1—N2—K2^{ii}	−71.8 (4)	K2—N2—C3—N3	−70.4 (3)
K1—N1—N2—K2^{ii}	18.4 (3)	K2^{ii}—N2—C3—N3	27.4 (4)
K2^{ii}—O1—N3—O2	−179.3 (2)	C1—C2—C3—N2	−0.8 (4)
K1^{ix}—O1—N3—O2	4.9 (3)	C5—C2—C3—N2	175.4 (4)
K2^{ii}—O1—N3—C3	0.1 (4)	C1—C2—C3—N3	179.0 (4)
K1^{ix}—O1—N3—C3	−175.7 (3)	C5—C2—C3—N3	−4.8 (6)
K2^{ii}—O1—N3—K1^{ix}	175.8 (2)	O1—N3—C3—N2	−18.3 (5)
K1^{ix}—O2—N3—O1	−5.9 (4)	O2—N3—C3—N2	161.1 (3)
K1^{vi}—O2—N3—O1	76.2 (4)	K1^{ix}—N3—C3—N2	−175.5 (10)
K1^{ix}—O2—N3—C3	174.8 (2)	O1—N3—C3—C2	161.9 (3)
K1^{vi}—O2—N3—C3	−103.1 (3)	O2—N3—C3—C2	−18.7 (5)
K1^{vi}—O2—N3—K1^{ix}	82.07 (14)	K1^{ix}—N3—C3—C2	4.6 (15)
C4—N4—N5—C6	−1.6 (4)	N5—N4—C4—C5	1.1 (4)
K2^{xi}—N4—N5—C6	147.6 (2)	K2^{xi}—N4—C4—C5	−155.2 (2)
K2^{xii}—N4—N5—C6	−127.3 (2)	K2^{xii}—N4—C4—C5	113.8 (3)
K1^{xii}—N4—N5—C6	130.0 (2)	K1^{xii}—N4—C4—C5	−65.2 (4)
C4—N4—N5—K1^{x}	143.1 (2)	N4—C4—C5—C6	−0.1 (4)
K2^{xi}—N4—N5—K1^{x}	−67.6 (3)	N4—C4—C5—C2	−175.9 (4)
K2^{xii}—N4—N5—K1^{x}	17.4 (2)	C1—C2—C5—C4	−140.9 (4)
K1^{xii}—N4—N5—K1^{x}	−85.21 (19)	C3—C2—C5—C4	43.9 (6)
C4—N4—N5—K1^{xii}	−131.7 (2)	C1—C2—C5—C6	44.5 (6)
K2^{xi}—N4—N5—K1^{xii}	17.6 (3)	C3—C2—C5—C6	−130.8 (4)
K2^{xii}—N4—N5—K1^{xii}	102.65 (9)	N4—N5—C6—C5	1.7 (4)
C4—N4—N5—K2^{xii}	125.7 (3)	K1^{x}—N5—C6—C5	−148.0 (2)
K2^{xi}—N4—N5—K2^{xii}	−85.1 (2)	K1^{xii}—N5—C6—C5	110.3 (3)
K1^{xii}—N4—N5—K2^{xii}	−102.65 (9)	K2^{xii}—N5—C6—C5	−59.2 (4)
K1^{x}—O3—N6—O4	178.3 (2)	N4—N5—C6—N6	−178.9 (3)
K2^{v}—O3—N6—O4	11.6 (3)	K1^{x}—N5—C6—N6	31.5 (3)
K1^{x}—O3—N6—C6	−2.1 (4)	K1^{xii}—N5—C6—N6	−70.3 (3)
K2^{v}—O3—N6—C6	−168.8 (2)	K2^{xii}—N5—C6—N6	120.2 (3)
K1^{x}—O3—N6—K2^{v}	166.7 (2)	C4—C5—C6—N5	−1.0 (4)
K2^{v}—O4—N6—O3	−13.3 (3)	C2—C5—C6—N5	174.8 (3)
K2^{i}—O4—N6—O3	73.7 (3)	C4—C5—C6—N6	179.7 (3)
K2^{v}—O4—N6—C6	167.1 (2)	C2—C5—C6—N6	−4.5 (7)
K2^{i}—O4—N6—C6	−105.9 (2)	O3—N6—C6—N5	−20.5 (4)
K2^{i}—O4—N6—K2^{v}	87.01 (13)	O4—N6—C6—N5	159.2 (3)
N2—N1—C1—C2	0.6 (4)	K2^{v}—N6—C6—N5	−146.9 (7)
K1^{viii}—N1—C1—C2	−148.5 (2)	O3—N6—C6—C5	158.9 (3)
K1—N1—C1—C2	117.4 (3)	O4—N6—C6—C5	−21.5 (5)
N1—C1—C2—C3	0.1 (4)	K2^{v}—N6—C6—C5	32.4 (11)

Symmetry codes: (i) −*x*+1/2, *y*, *z*−1/2; (ii) *x*, *y*−1, *z*; (iii) *x*+1/2, −*y*−1, *z*; (iv) *x*+1/2, −*y*, *z*; (v) −*x*+1/2, *y*−1, *z*−1/2; (vi) −*x*+1/2, *y*+1, *z*+1/2; (vii) *x*+1/2, −*y*+1, *z*; (viii) *x*, *y*+1, *z*; (ix) −*x*+1/2, *y*, *z*+1/2; (x) *x*−1/2, −*y*−1, *z*; (xi) *x*−1/2, −*y*+1, *z*; (xii) *x*−1/2, −*y*, *z*.

Hydrogen-bond geometry (Å, º)

D—H···*A*	*D*—H	H···*A*	*D*···*A*	*D*—H···*A*
C4—H4···O3^{xiii}	0.94	2.62	3.352 (4)	135

Symmetry code: (xiii) −*x*, −*y*, *z*+1/2.

Poly[[*μ*-3,3′-dinitro-4,4′-bipyrazole-1,1′-diido]dirubidium] (2)

Crystal data

$[Rb_2(C_6H_2N_6O_4)]$
M_r = 393.08
Monoclinic, $P2_1/n$
a = 3.9669 (2) Å
b = 14.2020 (4) Å
c = 18.6685 (6) Å
β = 95.776 (3)°
V = 1046.40 (7) Å^3
Z = 4
$F(000)$ = 744
D_x = 2.495 Mg m^{-3}
Cu $K\alpha$ radiation, λ = 1.54186 Å
Cell parameters from 10655 reflections
θ = 3.9–79.9°
μ = 12.38 mm^{-1}
T = 173 K
Prism, red
0.05 × 0.03 × 0.03 mm

Data collection

Stoe Stadivari diffractometer
Radiation source: GeniX 3D HF Cu
Graded multilayer mirror monochromator
Detector resolution: 5.81 pixels mm^{-1}
rotation method, ω scans
Absorption correction: multi-scan (Stoe *LANA*; Koziskova *et al.*, 2016)
T_{min} = 0.469, T_{max} = 0.661
10655 measured reflections
2234 independent reflections
2156 reflections with $I > 2\sigma(I)$
R_{int} = 0.030
θ_{max} = 79.9°, θ_{min} = 3.9°
h = −4→5
k = −16→18
l = −23→13

Refinement

Refinement on F^2
Least-squares matrix: full
$R[F^2 > 2\sigma(F^2)]$ = 0.048
$wR(F^2)$ = 0.148
S = 1.14
2234 reflections
164 parameters
0 restraints
Primary atom site location: structure-invariant direct methods
Secondary atom site location: difference Fourier map
Hydrogen site location: inferred from neighbouring sites
H-atom parameters constrained
$w = 1/[\sigma^2(F_o^2) + (0.1033P)^2 + 1.4588P]$ where $P = (F_o^2 + 2F_c^2)/3$
$(\Delta/\sigma)_{max} < 0.001$
$\Delta\rho_{max}$ = 0.86 e Å^{-3}
$\Delta\rho_{min}$ = −0.72 e Å^{-3}
Extinction correction: SHELXL-2019/2 (Sheldrick 2015), $Fc^*=kFc[1+0.001xFc^2\lambda^3/\sin(2\theta)]^{-1/4}$
Extinction coefficient: 0.0053 (6)

Special details

Geometry. All esds (except the esd in the dihedral angle between two l.s. planes) are estimated using the full covariance matrix. The cell esds are taken into account individually in the estimation of esds in distances, angles and torsion angles; correlations between esds in cell parameters are only used when they are defined by crystal symmetry. An approximate (isotropic) treatment of cell esds is used for estimating esds involving l.s. planes.

Fractional atomic coordinates and isotropic or equivalent isotropic displacement parameters (Å^2)

	x	*y*	*z*	U_{iso}*/U_{eq}
Rb1	0.45494 (11)	0.14140 (3)	0.16029 (2)	0.0392 (2)

Rb2	0.58119 (11)	0.41180 (3)	0.12337 (2)	0.0362 (2)
O1	0.7633 (14)	0.0654 (3)	0.4780 (2)	0.0632 (13)
O2	0.4337 (10)	0.0869 (2)	0.38057 (19)	0.0455 (9)
O3	0.5123 (11)	0.5029 (3)	0.2664 (2)	0.0462 (8)
O4	0.6039 (13)	0.4655 (3)	0.3786 (2)	0.0551 (10)
N1	0.4128 (11)	0.3078 (3)	0.5487 (2)	0.0402 (9)
N2	0.5224 (10)	0.2195 (3)	0.5384 (2)	0.0365 (8)
N3	0.5540 (11)	0.1145 (3)	0.4407 (2)	0.0393 (8)
N4	−0.0293 (10)	0.2675 (3)	0.2376 (2)	0.0380 (8)
N5	0.1348 (11)	0.3503 (3)	0.2363 (2)	0.0369 (8)
N6	0.4738 (11)	0.4480 (3)	0.3171 (2)	0.0377 (8)
C1	0.2944 (14)	0.3447 (4)	0.4844 (3)	0.0402 (10)
H1	0.208345	0.406910	0.477873	0.048*
C2	0.3144 (12)	0.2798 (3)	0.4285 (2)	0.0357 (9)
C3	0.4585 (11)	0.2026 (3)	0.4670 (2)	0.0345 (9)
C4	0.0201 (13)	0.2325 (3)	0.3057 (2)	0.0376 (9)
H4	−0.068538	0.174024	0.319981	0.045*
C5	0.2154 (11)	0.2923 (3)	0.3518 (2)	0.0344 (9)
C6	0.2779 (12)	0.3658 (3)	0.3039 (2)	0.0348 (9)

Atomic displacement parameters (Å²)

	U^{11}	U^{22}	U^{33}	U^{12}	U^{13}	U^{23}
Rb1	0.0390 (3)	0.0381 (3)	0.0404 (3)	−0.00137 (15)	0.0037 (2)	0.00171 (16)
Rb2	0.0402 (3)	0.0377 (3)	0.0304 (3)	−0.00063 (15)	0.0022 (2)	0.00187 (14)
O1	0.084 (3)	0.052 (2)	0.048 (2)	0.029 (2)	−0.023 (2)	−0.0114 (18)
O2	0.059 (2)	0.0404 (19)	0.0355 (19)	0.0052 (14)	−0.0054 (17)	−0.0062 (13)
O3	0.062 (2)	0.0378 (17)	0.0398 (19)	−0.0062 (15)	0.0081 (16)	0.0001 (14)
O4	0.081 (3)	0.048 (2)	0.0340 (18)	−0.0181 (19)	−0.0040 (17)	0.0008 (15)
N1	0.049 (2)	0.041 (2)	0.0309 (19)	0.0016 (17)	0.0047 (16)	−0.0012 (15)
N2	0.0413 (19)	0.0389 (19)	0.0291 (17)	0.0016 (15)	0.0028 (14)	0.0023 (15)
N3	0.042 (2)	0.039 (2)	0.036 (2)	0.0027 (17)	0.0001 (16)	−0.0006 (16)
N4	0.040 (2)	0.043 (2)	0.0309 (18)	−0.0046 (16)	0.0015 (15)	−0.0033 (15)
N5	0.038 (2)	0.042 (2)	0.0306 (19)	0.0019 (15)	−0.0001 (15)	0.0029 (14)
N6	0.047 (2)	0.0336 (18)	0.0325 (19)	0.0019 (16)	0.0056 (16)	−0.0013 (15)
C1	0.052 (3)	0.039 (2)	0.029 (2)	0.006 (2)	0.0005 (19)	−0.0017 (17)
C2	0.042 (2)	0.033 (2)	0.032 (2)	0.0000 (17)	0.0021 (17)	0.0007 (17)
C3	0.036 (2)	0.036 (2)	0.030 (2)	−0.0015 (17)	0.0008 (16)	0.0014 (16)
C4	0.047 (2)	0.037 (2)	0.029 (2)	0.0017 (18)	0.0019 (18)	0.0003 (17)
C5	0.037 (2)	0.036 (2)	0.030 (2)	0.0036 (16)	0.0013 (16)	0.0004 (16)
C6	0.038 (2)	0.038 (2)	0.029 (2)	0.0017 (16)	0.0037 (17)	0.0017 (16)

Geometric parameters (Å, º)

Rb1—N1^{i}	2.930 (4)	O2—N3	1.238 (5)
Rb1—N4^{ii}	2.980 (4)	O3—N6	1.247 (5)
Rb1—N1^{iii}	2.987 (4)	O4—N6	1.235 (6)
Rb1—N4	3.088 (4)	N1—N2	1.347 (6)

Rb1—O3^{iv}	3.103 (4)	N1—C1	1.350 (6)
Rb1—O3^{v}	3.113 (4)	N2—C3	1.353 (6)
Rb1—O4^{iv}	3.175 (4)	N3—C3	1.410 (6)
Rb1—O4^{v}	3.370 (5)	N4—N5	1.345 (6)
Rb2—O1^{i}	2.893 (4)	N4—C4	1.361 (6)
Rb2—O1^{vi}	2.993 (4)	N5—C6	1.348 (6)
Rb2—O3	3.004 (4)	N6—C6	1.410 (6)
Rb2—N5	3.016 (4)	C1—C2	1.401 (6)
Rb2—N5^{ii}	3.017 (4)	C1—H1	0.9500
Rb2—N2^{iii}	3.101 (4)	C2—C3	1.401 (6)
Rb2—O2^{vi}	3.150 (4)	C2—C5	1.456 (6)
Rb2—N2^{i}	3.194 (4)	C4—C5	1.389 (6)
Rb2—O2^{vii}	3.214 (4)	C4—H4	0.9500
O1—N3	1.243 (6)	C5—C6	1.413 (6)

N1^{i}—Rb1—N4^{ii}	127.98 (12)	N6—O3—Rb1^{vii}	86.4 (3)
N1^{i}—Rb1—N1^{iii}	84.19 (10)	Rb2—O3—Rb1^{vii}	140.74 (14)
N4^{ii}—Rb1—N1^{iii}	75.92 (11)	Rb1^{vi}—O3—Rb1^{vii}	79.32 (9)
N1^{i}—Rb1—N4	75.11 (11)	N6—O4—Rb1^{vi}	97.8 (3)
N4^{ii}—Rb1—N4	81.61 (10)	N6—O4—Rb1^{vii}	75.3 (3)
N1^{iii}—Rb1—N4	129.52 (11)	Rb1^{vi}—O4—Rb1^{vii}	74.55 (8)
N1^{i}—Rb1—O3^{iv}	152.66 (11)	N2—N1—C1	108.9 (4)
N4^{ii}—Rb1—O3^{iv}	76.33 (11)	N2—N1—Rb1^{viii}	96.1 (3)
N1^{iii}—Rb1—O3^{iv}	91.48 (11)	C1—N1—Rb1^{viii}	134.5 (3)
N4—Rb1—O3^{iv}	126.14 (10)	N2—N1—Rb1^{ix}	123.5 (3)
N1^{i}—Rb1—O3^{v}	92.37 (11)	C1—N1—Rb1^{ix}	110.2 (3)
N4^{ii}—Rb1—O3^{v}	125.25 (10)	Rb1^{viii}—N1—Rb1^{ix}	84.18 (10)
N1^{iii}—Rb1—O3^{v}	152.88 (10)	N1—N2—C3	105.9 (4)
N4—Rb1—O3^{v}	74.65 (10)	N1—N2—Rb2^{ix}	106.3 (3)
O3^{iv}—Rb1—O3^{v}	79.32 (9)	C3—N2—Rb2^{ix}	109.8 (3)
N1^{i}—Rb1—O4^{iv}	114.40 (11)	N1—N2—Rb2^{viii}	133.7 (3)
N4^{ii}—Rb1—O4^{iv}	102.48 (12)	C3—N2—Rb2^{viii}	116.0 (3)
N1^{iii}—Rb1—O4^{iv}	69.07 (12)	Rb2^{ix}—N2—Rb2^{viii}	78.11 (9)
N4—Rb1—O4^{iv}	161.07 (11)	N1—N2—Rb1^{viii}	60.4 (2)
O3^{iv}—Rb1—O4^{iv}	40.13 (9)	C3—N2—Rb1^{viii}	143.7 (3)
O3^{v}—Rb1—O4^{iv}	88.25 (11)	Rb2^{ix}—N2—Rb1^{viii}	106.49 (11)
N1^{i}—Rb1—O4^{v}	67.01 (10)	Rb2^{viii}—N2—Rb1^{viii}	74.02 (8)
N4^{ii}—Rb1—O4^{v}	162.62 (10)	O2—N3—O1	120.4 (4)
N1^{iii}—Rb1—O4^{v}	117.51 (11)	O2—N3—C3	120.3 (4)
N4—Rb1—O4^{v}	95.96 (11)	O1—N3—C3	119.3 (4)
O3^{iv}—Rb1—O4^{v}	91.67 (10)	O2—N3—Rb2^{iv}	64.1 (2)
O3^{v}—Rb1—O4^{v}	38.57 (9)	O1—N3—Rb2^{iv}	56.8 (3)
O4^{iv}—Rb1—O4^{v}	74.55 (8)	C3—N3—Rb2^{iv}	170.9 (3)
O1^{i}—Rb2—O1^{vi}	54.79 (14)	N5—N4—C4	108.2 (4)
O1^{i}—Rb2—O3	135.69 (14)	N5—N4—Rb1^{x}	145.7 (3)
O1^{vi}—Rb2—O3	106.93 (12)	C4—N4—Rb1^{x}	105.0 (3)
O1^{i}—Rb2—N5	117.20 (13)	N5—N4—Rb1	100.0 (3)
O1^{vi}—Rb2—N5	145.70 (14)	C4—N4—Rb1	100.8 (3)

O3—Rb2—N5	52.47 (11)	Rb1^{x}—N4—Rb1	81.61 (10)
O1^{i}—Rb2—N5^{ii}	154.94 (14)	N5—N4—Rb2^{x}	68.6 (2)
O1^{vi}—Rb2—N5^{ii}	118.11 (12)	C4—N4—Rb2^{x}	149.5 (3)
O3—Rb2—N5^{ii}	68.18 (11)	Rb1^{x}—N4—Rb2^{x}	78.61 (9)
N5—Rb2—N5^{ii}	82.23 (10)	Rb1—N4—Rb2^{x}	109.73 (11)
O1^{i}—Rb2—N2^{iii}	78.61 (14)	N4—N5—C6	106.6 (4)
O1^{vi}—Rb2—N2^{iii}	87.26 (14)	N4—N5—Rb2	125.8 (3)
O3—Rb2—N2^{iii}	145.10 (11)	C6—N5—Rb2	112.7 (3)
N5—Rb2—N2^{iii}	125.79 (11)	N4—N5—Rb2^{x}	86.9 (3)
N5^{ii}—Rb2—N2^{iii}	76.98 (11)	C6—N5—Rb2^{x}	144.6 (3)
O1^{i}—Rb2—O2^{vi}	95.71 (10)	Rb2—N5—Rb2^{x}	82.23 (10)
O1^{vi}—Rb2—O2^{vi}	40.92 (10)	O4—N6—O3	120.5 (4)
O3—Rb2—O2^{vi}	77.95 (10)	O4—N6—C6	120.1 (4)
N5—Rb2—O2^{vi}	130.39 (11)	O3—N6—C6	119.4 (4)
N5^{ii}—Rb2—O2^{vi}	80.87 (10)	O4—N6—Rb1^{vii}	83.4 (3)
N2^{iii}—Rb2—O2^{vi}	94.89 (11)	O3—N6—Rb1^{vii}	71.3 (3)
O1^{i}—Rb2—N2^{i}	51.99 (11)	C6—N6—Rb1^{vii}	115.6 (3)
O1^{vi}—Rb2—N2^{i}	106.77 (10)	O4—N6—Rb1^{vi}	62.1 (3)
O3—Rb2—N2^{i}	124.90 (11)	O3—N6—Rb1^{vi}	58.8 (2)
N5—Rb2—N2^{i}	75.59 (11)	C6—N6—Rb1^{vi}	173.1 (3)
N5^{ii}—Rb2—N2^{i}	126.74 (11)	Rb1^{vii}—N6—Rb1^{vi}	70.77 (8)
N2^{iii}—Rb2—N2^{i}	78.11 (9)	N1—C1—C2	111.5 (4)
O2^{vi}—Rb2—N2^{i}	147.62 (9)	N1—C1—H1	124.3
O1^{i}—Rb2—O2^{vii}	71.10 (13)	C2—C1—H1	124.3
O1^{vi}—Rb2—O2^{vii}	65.94 (13)	C1—C2—C3	100.5 (4)
O3—Rb2—O2^{vii}	64.71 (10)	C1—C2—C5	128.5 (4)
N5—Rb2—O2^{vii}	79.84 (10)	C3—C2—C5	131.0 (4)
N5^{ii}—Rb2—O2^{vii}	131.02 (10)	N2—C3—C2	113.2 (4)
N2^{iii}—Rb2—O2^{vii}	147.53 (10)	N2—C3—N3	118.1 (4)
O2^{vi}—Rb2—O2^{vii}	77.11 (8)	C2—C3—N3	128.7 (4)
N2^{i}—Rb2—O2^{vii}	91.88 (10)	N4—C4—C5	112.0 (4)
N3—O1—Rb2^{viii}	131.8 (3)	N4—C4—H4	124.0
N3—O1—Rb2^{iv}	102.9 (3)	C5—C4—H4	124.0
Rb2^{viii}—O1—Rb2^{iv}	125.21 (14)	C4—C5—C6	100.5 (4)
N3—O2—Rb2^{iv}	95.2 (3)	C4—C5—C2	127.8 (4)
N3—O2—Rb2^{v}	116.9 (3)	C6—C5—C2	131.7 (4)
Rb2^{iv}—O2—Rb2^{v}	77.11 (8)	N5—C6—N6	118.2 (4)
N6—O3—Rb2	115.7 (3)	N5—C6—C5	112.8 (4)
N6—O3—Rb1^{vi}	101.0 (3)	N6—C6—C5	129.0 (4)
Rb2—O3—Rb1^{vi}	123.10 (13)		

C1—N1—N2—C3	−1.9 (5)	Rb1^{ix}—N1—C1—C2	−136.8 (4)
Rb1^{viii}—N1—N2—C3	−143.3 (3)	N1—C1—C2—C5	−179.6 (5)
Rb1^{ix}—N1—N2—C3	129.7 (3)	N1—N2—C3—C2	1.6 (5)
C1—N1—N2—Rb2^{ix}	−118.5 (4)	Rb2^{ix}—N2—C3—C2	115.9 (4)
Rb1^{viii}—N1—N2—Rb2^{ix}	100.03 (16)	Rb2^{viii}—N2—C3—C2	−158.0 (3)
Rb1^{ix}—N1—N2—Rb2^{ix}	13.0 (4)	Rb1^{viii}—N2—C3—C2	−59.7 (6)
C1—N1—N2—Rb2^{viii}	152.5 (4)	N1—N2—C3—N3	179.0 (4)

Rb1^{viii}—N1—N2—Rb2^{viii}	11.1 (4)	Rb2^{ix}—N2—C3—N3	−66.7 (4)
Rb1^{ix}—N1—N2—Rb2^{viii}	−76.0 (4)	Rb2^{viii}—N2—C3—N3	19.4 (5)
C1—N1—N2—Rb1^{viii}	141.4 (4)	Rb1^{viii}—N2—C3—N3	117.7 (5)
Rb1^{ix}—N1—N2—Rb1^{viii}	−87.0 (3)	C1—C2—C3—N2	−0.7 (6)
Rb2^{iv}—O2—N3—O1	−8.1 (5)	C5—C2—C3—N2	178.4 (5)
Rb2^{v}—O2—N3—O1	70.1 (6)	C1—C2—C3—N3	−177.8 (5)
Rb2^{iv}—O2—N3—C3	171.0 (4)	C5—C2—C3—N3	1.3 (9)
Rb2^{v}—O2—N3—C3	−110.9 (4)	O2—N3—C3—N2	163.0 (4)
Rb2^{v}—O2—N3—Rb2^{iv}	78.17 (18)	O1—N3—C3—N2	−17.9 (7)
Rb2^{viii}—O1—N3—O2	−174.8 (4)	O2—N3—C3—C2	−20.0 (8)
Rb2^{iv}—O1—N3—O2	8.7 (6)	O1—N3—C3—C2	159.1 (5)
Rb2^{viii}—O1—N3—C3	6.1 (8)	N5—N4—C4—C5	0.9 (6)
Rb2^{iv}—O1—N3—C3	−170.4 (3)	Rb1^{x}—N4—C4—C5	−170.6 (3)
Rb2^{viii}—O1—N3—Rb2^{iv}	176.5 (6)	Rb1—N4—C4—C5	105.3 (4)
C4—N4—N5—C6	−1.0 (5)	Rb2^{x}—N4—C4—C5	−77.6 (7)
Rb1^{x}—N4—N5—C6	164.3 (4)	N5—N4—C4—Rb1^{x}	171.5 (4)
Rb1—N4—N5—C6	−106.0 (3)	Rb1—N4—C4—Rb1^{x}	−84.11 (17)
Rb2^{x}—N4—N5—C6	146.6 (4)	Rb2^{x}—N4—C4—Rb1^{x}	93.1 (6)
C4—N4—N5—Rb2	134.2 (3)	N5—N4—C4—Rb1	−104.4 (4)
Rb1^{x}—N4—N5—Rb2	−60.5 (6)	Rb1^{x}—N4—C4—Rb1	84.11 (17)
Rb1—N4—N5—Rb2	29.3 (3)	Rb2^{x}—N4—C4—Rb1	177.2 (7)
Rb2^{x}—N4—N5—Rb2	−78.1 (2)	N4—C4—C5—C6	−0.4 (5)
C4—N4—N5—Rb2^{x}	−147.7 (3)	N4—C4—C5—C2	178.5 (4)
Rb1^{x}—N4—N5—Rb2^{x}	17.6 (5)	C1—C2—C5—C4	−131.9 (6)
Rb1—N4—N5—Rb2^{x}	107.40 (13)	C3—C2—C5—C4	49.3 (8)
Rb1^{vi}—O4—N6—O3	−8.0 (5)	C1—C2—C5—C6	46.6 (8)
Rb1^{vii}—O4—N6—O3	63.7 (4)	C3—C2—C5—C6	−132.2 (6)
Rb1^{vi}—O4—N6—C6	172.5 (4)	N4—N5—C6—N6	178.6 (4)
Rb1^{vii}—O4—N6—C6	−115.8 (4)	Rb2—N5—C6—N6	36.8 (5)
Rb1^{vi}—O4—N6—Rb1^{vii}	−71.71 (13)	Rb2^{x}—N5—C6—N6	−72.7 (7)
Rb1^{vii}—O4—N6—Rb1^{vi}	71.71 (13)	N4—N5—C6—C5	0.9 (5)
Rb2—O3—N6—O4	143.7 (4)	Rb2—N5—C6—C5	−140.9 (3)
Rb1^{vi}—O3—N6—O4	8.3 (5)	Rb2^{x}—N5—C6—C5	109.6 (5)
Rb1^{vii}—O3—N6—O4	−70.1 (5)	O4—N6—C6—N5	178.7 (5)
Rb2—O3—N6—C6	−36.8 (5)	O3—N6—C6—N5	−0.8 (7)
Rb1^{vi}—O3—N6—C6	−172.2 (3)	Rb1^{vii}—N6—C6—N5	81.2 (4)
Rb1^{vii}—O3—N6—C6	109.4 (4)	O4—N6—C6—C5	−4.0 (8)
Rb2—O3—N6—Rb1^{vii}	−146.2 (3)	O3—N6—C6—C5	176.5 (5)
Rb1^{vi}—O3—N6—Rb1^{vii}	78.39 (12)	Rb1^{vii}—N6—C6—C5	−101.5 (5)
Rb2—O3—N6—Rb1^{vi}	135.4 (3)	C4—C5—C6—N5	−0.3 (5)
Rb1^{vii}—O3—N6—Rb1^{vi}	−78.39 (12)	C2—C5—C6—N5	−179.1 (5)
N2—N1—C1—C2	1.5 (6)	C4—C5—C6—N6	−177.7 (5)
Rb1^{viii}—N1—C1—C2	121.1 (4)	C2—C5—C6—N6	3.5 (8)

Symmetry codes: (i) $x-1/2, -y+1/2, z-1/2$; (ii) $x+1, y, z$; (iii) $x+1/2, -y+1/2, z-1/2$; (iv) $-x+3/2, y-1/2, -z+1/2$; (v) $-x+1/2, y-1/2, -z+1/2$; (vi) $-x+3/2, y+1/2, -z+1/2$; (vii) $-x+1/2, y+1/2, -z+1/2$; (viii) $x+1/2, -y+1/2, z+1/2$; (ix) $x-1/2, -y+1/2, z+1/2$; (x) $x-1, y, z$.

Hydrogen-bond geometry (Å, º)

D—H···*A*	*D*—H	H···*A*	*D*···*A*	*D*—H···*A*
C4—H4···O2^{x}	0.95	2.68	3.506 (6)	146

Symmetry code: (x) *x*−1, *y*, *z*.

Poly[[[*μ*-3,3′-dinitro-4,4′-bipyrazole-1,1′-diido]dicaesium] monohydrate] (3)

Crystal data

$[Cs_2(C_6H_2N_6O_4)]\cdot H_2O$
M_r = 505.97
Monoclinic, $P2_1$
a = 9.7388 (7) Å
b = 6.9551 (3) Å
c = 10.2950 (7) Å
β = 118.152 (8)°
V = 614.83 (8) Å^3
Z = 2
$F(000)$ = 464
D_x = 2.733 Mg m^{-3}
Mo $K\alpha$ radiation, λ = 0.71073 Å
Cell parameters from 4971 reflections
θ = 2.4–27.1°
μ = 5.96 mm^{-1}
T = 213 K
Prism, red
0.20 × 0.17 × 0.14 mm

Data collection

Stoe Image plate diffraction system-2T diffractometer
Radiation source: fine-focus sealed tube
φ oscillation scans
Absorption correction: numerical [X-RED (Stoe & Cie, 2001) and X-SHAPE (Stoe & Cie, 1999)]
T_{min} = 0.218, T_{max} = 0.245
4971 measured reflections
2554 independent reflections
2376 reflections with $I > 2\sigma(I)$
R_{int} = 0.020
θ_{max} = 27.1°, θ_{min} = 2.4°
h = −12→12
k = −8→8
l = −13→13

Refinement

Refinement on F^2
Least-squares matrix: full
$R[F^2 > 2\sigma(F^2)]$ = 0.020
$wR(F^2)$ = 0.045
S = 0.99
2554 reflections
173 parameters
1 restraint
Primary atom site location: structure-invariant direct methods
Secondary atom site location: difference Fourier map
Hydrogen site location: mixed
H-atom parameters constrained
$w = 1/[\sigma^2(F_o^2) + (0.0271P)^2]$ where $P = (F_o^2 + 2F_c^2)/3$
$(\Delta/\sigma)_{max} < 0.001$
$\Delta\rho_{max}$ = 0.93 e Å^{-3}
$\Delta\rho_{min}$ = −1.17 e Å^{-3}
Absolute structure: Refined as an inversion twin
Absolute structure parameter: 0.44 (3)

Special details

Geometry. All esds (except the esd in the dihedral angle between two l.s. planes) are estimated using the full covariance matrix. The cell esds are taken into account individually in the estimation of esds in distances, angles and torsion angles; correlations between esds in cell parameters are only used when they are defined by crystal symmetry. An approximate (isotropic) treatment of cell esds is used for estimating esds involving l.s. planes.

Refinement. Refined as a 2-component inversion twin.

Fractional atomic coordinates and isotropic or equivalent isotropic displacement parameters (Å^2)

	x	*y*	*z*	U_{iso}*/U_{eq}
Cs1	0.37557 (4)	−0.01332 (6)	0.83234 (4)	0.02622 (11)

Cs2	0.28594 (4)	0.21708 (6)	0.40418 (4)	0.02770 (11)
O1	0.2933 (5)	0.6346 (8)	0.9720 (6)	0.0378 (13)
O2	0.0596 (6)	0.6050 (9)	0.7982 (7)	0.0550 (19)
O3	−0.0531 (7)	0.3586 (11)	0.4159 (6)	0.058 (2)
O4	0.1297 (5)	0.2870 (10)	0.6288 (6)	0.0460 (17)
N1	0.2513 (6)	0.0986 (9)	1.0846 (6)	0.0256 (13)
N2	0.2885 (6)	0.2776 (9)	1.0688 (5)	0.0225 (12)
N3	0.1744 (6)	0.5375 (9)	0.9019 (6)	0.0281 (15)
N4	−0.3494 (6)	0.2071 (11)	0.5665 (6)	0.0302 (13)
N5	−0.2719 (5)	0.2515 (10)	0.4893 (5)	0.0270 (13)
N6	−0.0093 (6)	0.3032 (10)	0.5416 (6)	0.0279 (13)
C1	0.1092 (7)	0.0551 (11)	0.9684 (7)	0.0245 (14)
H1	0.057551	−0.063088	0.955557	0.029*
C2	0.0521 (5)	0.2089 (11)	0.8725 (6)	0.0177 (11)
C3	0.1704 (7)	0.3440 (10)	0.9432 (7)	0.0211 (13)
C4	−0.2440 (7)	0.1895 (11)	0.7100 (7)	0.0241 (15)
H4	−0.269184	0.160356	0.785344	0.029*
C5	−0.0932 (6)	0.2199 (11)	0.7323 (6)	0.0201 (11)
C6	−0.1201 (6)	0.2587 (10)	0.5895 (6)	0.0218 (14)
O1W	0.4552 (6)	0.4093 (9)	0.7600 (7)	0.0527 (18)
H1W	0.546627	0.455957	0.802129	0.079*
H2W	0.395147	0.489868	0.696509	0.079*

Atomic displacement parameters (Å²)

	U^{11}	U^{22}	U^{33}	U^{12}	U^{13}	U^{23}
Cs1	0.01693 (17)	0.0311 (3)	0.02732 (19)	0.00105 (17)	0.00772 (14)	−0.00028 (19)
Cs2	0.01801 (17)	0.0343 (3)	0.0277 (2)	−0.00397 (19)	0.00824 (14)	0.00034 (19)
O1	0.021 (2)	0.026 (3)	0.051 (3)	−0.008 (2)	0.005 (2)	0.002 (2)
O2	0.033 (3)	0.026 (4)	0.067 (4)	−0.001 (2)	−0.010 (3)	0.016 (3)
O3	0.035 (3)	0.105 (6)	0.031 (3)	0.006 (3)	0.012 (2)	0.022 (3)
O4	0.017 (2)	0.081 (5)	0.040 (3)	0.005 (2)	0.013 (2)	0.022 (3)
N1	0.024 (3)	0.026 (4)	0.026 (3)	0.000 (2)	0.011 (2)	0.003 (2)
N2	0.018 (2)	0.025 (4)	0.020 (2)	0.002 (2)	0.006 (2)	0.000 (2)
N3	0.017 (2)	0.027 (5)	0.031 (3)	0.002 (2)	0.003 (2)	0.004 (2)
N4	0.016 (2)	0.032 (4)	0.037 (3)	−0.005 (3)	0.007 (2)	−0.004 (3)
N5	0.015 (2)	0.034 (4)	0.025 (3)	0.004 (2)	0.0031 (19)	−0.003 (3)
N6	0.023 (3)	0.034 (4)	0.024 (3)	0.005 (2)	0.009 (2)	0.005 (2)
C1	0.020 (3)	0.029 (4)	0.026 (3)	−0.003 (3)	0.013 (3)	0.000 (3)
C2	0.010 (2)	0.021 (3)	0.021 (2)	0.001 (3)	0.0060 (19)	−0.001 (3)
C3	0.020 (3)	0.016 (4)	0.025 (3)	0.000 (2)	0.008 (3)	0.000 (3)
C4	0.019 (3)	0.021 (4)	0.032 (3)	−0.004 (3)	0.012 (2)	−0.002 (3)
C5	0.012 (2)	0.020 (3)	0.024 (3)	0.002 (3)	0.005 (2)	−0.004 (3)
C6	0.013 (2)	0.023 (4)	0.026 (3)	0.003 (2)	0.006 (2)	−0.001 (3)
O1W	0.024 (3)	0.049 (5)	0.065 (4)	−0.010 (3)	0.005 (3)	0.006 (3)

Geometric parameters (Å, º)

Cs1—O1^{i}	3.064 (5)	O3—N6	1.218 (7)
Cs1—O3^{ii}	3.101 (6)	O4—N6	1.227 (7)
Cs1—O4	3.123 (5)	N1—N2	1.328 (8)
Cs1—O1^{iii}	3.130 (6)	N1—C1	1.370 (8)
Cs1—O1W	3.215 (6)	N2—C3	1.344 (8)
Cs1—N2^{i}	3.273 (5)	N3—C3	1.417 (9)
Cs1—N5^{ii}	3.392 (6)	N4—C4	1.349 (8)
Cs1—Cg1	3.389 (3)	N4—N5	1.365 (8)
Cs1—O1W^{i}	3.754 (7)	N5—C6	1.346 (7)
Cs2—O2^{ii}	3.107 (5)	N6—C6	1.417 (8)
Cs2—N4^{iv}	3.132 (5)	C1—C2	1.382 (10)
Cs2—N1^{v}	3.251 (6)	C1—H1	0.9400
Cs2—O4	3.350 (5)	C2—C3	1.396 (9)
Cs2—O1W	3.496 (7)	C2—C5	1.471 (7)
Cs2—O3	3.502 (6)	C4—C5	1.391 (8)
Cs2—Cg2^{ii}	3.474 (3)	C4—H4	0.9400
Cs2—Cg2^{vi}	3.587 (3)	C5—C6	1.392 (8)
O1—N3	1.236 (7)	O1W—H1W	0.8500
O2—N3	1.219 (7)	O1W—H2W	0.8500

O1^{i}—Cs1—O3^{ii}	168.81 (16)	N6—O4—Cs2	102.2 (4)
O1^{i}—Cs1—O4	116.91 (15)	Cs1—O4—Cs2	84.94 (13)
O3^{ii}—Cs1—O4	58.76 (19)	N2—N1—C1	108.7 (5)
O1^{i}—Cs1—O1^{iii}	112.27 (11)	N2—N1—Cs2^{ix}	89.0 (4)
O3^{ii}—Cs1—O1^{iii}	76.97 (17)	C1—N1—Cs2^{ix}	121.3 (4)
O4—Cs1—O1^{iii}	123.38 (13)	N1—N2—C3	106.3 (5)
O1^{i}—Cs1—O1W	63.35 (14)	N1—N2—Cs1^{vii}	132.0 (4)
O3^{ii}—Cs1—O1W	109.44 (18)	C3—N2—Cs1^{vii}	115.0 (4)
O4—Cs1—O1W	54.93 (14)	N1—N2—Cs2^{ix}	68.6 (3)
O1^{iii}—Cs1—O1W	164.51 (17)	C3—N2—Cs2^{ix}	126.2 (4)
O1^{i}—Cs1—N2^{i}	49.99 (14)	Cs1^{vii}—N2—Cs2^{ix}	102.63 (13)
O3^{ii}—Cs1—N2^{i}	127.14 (16)	O2—N3—O1	121.4 (7)
O4—Cs1—N2^{i}	147.49 (13)	O2—N3—C3	119.0 (6)
O1^{iii}—Cs1—N2^{i}	86.82 (14)	O1—N3—C3	119.6 (5)
O1W—Cs1—N2^{i}	99.40 (14)	C4—N4—N5	108.3 (5)
O1^{i}—Cs1—N5^{ii}	122.67 (14)	C4—N4—Cs2^{x}	132.2 (4)
O3^{ii}—Cs1—N5^{ii}	48.52 (14)	N5—N4—Cs2^{x}	118.9 (3)
O4—Cs1—N5^{ii}	83.50 (16)	C4—N4—Cs2^{ii}	78.6 (5)
O1^{iii}—Cs1—N5^{ii}	92.77 (15)	N5—N4—Cs2^{ii}	98.6 (4)
O1W—Cs1—N5^{ii}	102.00 (16)	Cs2^{x}—N4—Cs2^{ii}	100.36 (17)
N2^{i}—Cs1—N5^{ii}	83.26 (13)	C4—N4—Cs2^{vi}	89.2 (4)
O1^{i}—Cs1—O1W^{i}	62.76 (15)	N5—N4—Cs2^{vi}	72.8 (4)
O3^{ii}—Cs1—O1W^{i}	128.32 (15)	Cs2^{x}—N4—Cs2^{vi}	97.47 (18)
O4—Cs1—O1W^{i}	129.74 (14)	Cs2^{ii}—N4—Cs2^{vi}	162.17 (15)
O1^{iii}—Cs1—O1W^{i}	56.41 (14)	C6—N5—N4	105.7 (5)
O1W—Cs1—O1W^{i}	111.30 (16)	C6—N5—Cs1^{vi}	116.3 (4)

N2^{i}—Cs1—O1W^{i}	75.01 (13)	N4—N5—Cs1^{vi}	133.3 (4)
N5^{ii}—Cs1—O1W^{i}	142.53 (14)	C6—N5—Cs2^{vi}	85.1 (4)
O2^{ii}—Cs2—N4^{iv}	161.58 (18)	N4—N5—Cs2^{vi}	84.9 (4)
O2^{ii}—Cs2—N1^{v}	72.28 (17)	Cs1^{vi}—N5—Cs2^{vi}	79.57 (14)
N4^{iv}—Cs2—N1^{v}	94.85 (14)	O3—N6—O4	121.3 (6)
O2^{ii}—Cs2—O4	78.36 (17)	O3—N6—C6	119.8 (6)
N4^{iv}—Cs2—O4	113.88 (13)	O4—N6—C6	118.9 (5)
N1^{v}—Cs2—O4	150.63 (13)	N1—C1—C2	110.7 (6)
O2^{ii}—Cs2—N4^{vi}	113.52 (14)	N1—C1—H1	124.7
N4^{iv}—Cs2—N4^{vi}	82.18 (15)	C2—C1—H1	124.7
N1^{v}—Cs2—N4^{vi}	105.51 (14)	C1—C2—C3	101.2 (5)
O4—Cs2—N4^{vi}	85.25 (15)	C1—C2—C5	128.1 (6)
O2^{ii}—Cs2—O1W	128.63 (17)	C3—C2—C5	130.7 (6)
N4^{iv}—Cs2—O1W	66.05 (14)	N2—C3—C2	113.1 (6)
N1^{v}—Cs2—O1W	158.38 (13)	N2—C3—N3	118.9 (6)
O4—Cs2—O1W	50.52 (13)	C2—C3—N3	128.0 (6)
N4^{vi}—Cs2—O1W	63.54 (14)	N4—C4—C5	111.5 (6)
O2^{ii}—Cs2—O3	49.70 (17)	N4—C4—H4	124.3
N4^{iv}—Cs2—O3	146.93 (15)	C5—C4—H4	124.3
N1^{v}—Cs2—O3	117.19 (14)	Cs2^{ii}—C4—H4	92.3
O4—Cs2—O3	36.14 (12)	Cs2^{vi}—C4—H4	115.5
N4^{vi}—Cs2—O3	81.51 (15)	C4—C5—C6	101.3 (5)
O1W—Cs2—O3	80.93 (14)	C4—C5—C2	127.3 (5)
O2^{ii}—Cs2—N4^{ii}	84.12 (14)	C6—C5—C2	131.3 (5)
N4^{iv}—Cs2—N4^{ii}	79.99 (14)	N5—C6—C5	113.2 (5)
N1^{v}—Cs2—N4^{ii}	76.47 (14)	N5—C6—N6	118.8 (5)
O4—Cs2—N4^{ii}	101.65 (15)	C5—C6—N6	128.0 (5)
N4^{vi}—Cs2—N4^{ii}	162.17 (15)	Cs1—O1W—Cs2	81.21 (14)
O1W—Cs2—N4^{ii}	108.21 (14)	Cs1—O1W—Cs1^{vii}	84.20 (14)
O3—Cs2—N4^{ii}	113.76 (15)	Cs2—O1W—Cs1^{vii}	165.33 (19)
N3—O1—Cs1^{vii}	127.3 (4)	Cs1—O1W—H1W	122.7
N3—O1—Cs1^{viii}	122.1 (4)	Cs2—O1W—H1W	122.9
Cs1^{vii}—O1—Cs1^{viii}	98.42 (14)	Cs1^{vii}—O1W—H1W	64.7
N3—O2—Cs2^{vi}	160.1 (6)	Cs1—O1W—H2W	128.9
N6—O3—Cs1^{vi}	132.6 (4)	Cs2—O1W—H2W	68.5
N6—O3—Cs2	94.9 (4)	Cs1^{vii}—O1W—H2W	123.0
Cs1^{vi}—O3—Cs2	131.08 (18)	H1W—O1W—H2W	108.4
N6—O4—Cs1	141.7 (5)		

C1—N1—N2—C3	−0.3 (7)	C1—C2—C3—N3	−175.8 (6)
Cs2^{ix}—N1—N2—C3	−123.2 (4)	C5—C2—C3—N3	5.7 (11)
C1—N1—N2—Cs1^{vii}	−149.2 (4)	O2—N3—C3—N2	−171.2 (7)
Cs2^{ix}—N1—N2—Cs1^{vii}	87.9 (4)	O1—N3—C3—N2	8.3 (9)
C1—N1—N2—Cs2^{ix}	122.9 (5)	O2—N3—C3—C2	5.1 (10)
Cs2^{vi}—O2—N3—O1	−129.3 (13)	O1—N3—C3—C2	−175.4 (6)
Cs2^{vi}—O2—N3—C3	50.2 (19)	N5—N4—C4—C5	−0.5 (9)
Cs1^{vii}—O1—N3—O2	−159.5 (6)	Cs2^{x}—N4—C4—C5	−171.5 (5)
Cs1^{viii}—O1—N3—O2	−25.5 (10)	Cs2^{ii}—N4—C4—C5	94.8 (6)

Cs1^{vii}—O1—N3—C3	21.0 (9)	Cs2^{vi}—N4—C4—C5	−72.1 (6)
Cs1^{viii}—O1—N3—C3	155.0 (4)	N5—N4—C4—Cs2^{ii}	−95.3 (5)
C4—N4—N5—C6	0.3 (8)	Cs2^{x}—N4—C4—Cs2^{ii}	93.7 (6)
Cs2^{x}—N4—N5—C6	172.6 (4)	Cs2^{vi}—N4—C4—Cs2^{ii}	−166.94 (14)
Cs2^{ii}—N4—N5—C6	−80.5 (5)	N5—N4—C4—Cs2^{vi}	71.6 (5)
Cs2^{vi}—N4—N5—C6	83.5 (5)	Cs2^{x}—N4—C4—Cs2^{vi}	−99.3 (6)
C4—N4—N5—Cs1^{vi}	−153.7 (5)	Cs2^{ii}—N4—C4—Cs2^{vi}	166.94 (14)
Cs2^{x}—N4—N5—Cs1^{vi}	18.6 (8)	N4—C4—C5—C6	0.6 (8)
Cs2^{ii}—N4—N5—Cs1^{vi}	125.5 (4)	Cs2^{ii}—C4—C5—C6	81.9 (5)
Cs2^{vi}—N4—N5—Cs1^{vi}	−70.5 (5)	Cs2^{vi}—C4—C5—C6	−64.2 (5)
C4—N4—N5—Cs2^{vi}	−83.2 (6)	N4—C4—C5—C2	−178.6 (7)
Cs2^{x}—N4—N5—Cs2^{vi}	89.1 (4)	C1—C2—C5—C4	57.5 (11)
Cs2^{ii}—N4—N5—Cs2^{vi}	−163.97 (14)	C3—C2—C5—C4	−124.4 (8)
Cs1^{vi}—O3—N6—O4	−168.9 (6)	C1—C2—C5—C6	−121.4 (9)
Cs2—O3—N6—O4	24.2 (8)	C3—C2—C5—C6	56.7 (11)
Cs1^{vi}—O3—N6—C6	10.3 (11)	C1—C2—C5—Cs2^{vi}	153.5 (5)
Cs2—O3—N6—C6	−156.7 (6)	C3—C2—C5—Cs2^{vi}	−28.4 (7)
Cs1—O4—N6—O3	−123.2 (7)	C1—C2—C5—Cs2^{ii}	−12.3 (7)
Cs2—O4—N6—O3	−25.9 (8)	C3—C2—C5—Cs2^{ii}	165.8 (5)
Cs1—O4—N6—C6	57.6 (10)	N4—N5—C6—C5	0.1 (9)
Cs2—O4—N6—C6	155.0 (5)	Cs1^{vi}—N5—C6—C5	159.3 (5)
N2—N1—C1—C2	0.7 (7)	Cs2^{vi}—N5—C6—C5	83.4 (6)
Cs2^{ix}—N1—C1—C2	101.4 (5)	N4—N5—C6—N6	−179.7 (6)
N1—C1—C2—C3	−0.8 (7)	Cs1^{vi}—N5—C6—N6	−20.6 (8)
N1—C1—C2—C5	177.7 (5)	Cs2^{vi}—N5—C6—N6	−96.4 (6)
N1—N2—C3—C2	−0.3 (7)	C4—C5—C6—N5	−0.4 (8)
Cs1^{vii}—N2—C3—C2	154.7 (4)	C2—C5—C6—N5	178.7 (8)
Cs2^{ix}—N2—C3—C2	−75.4 (6)	C4—C5—C6—N6	179.4 (7)
N1—N2—C3—N3	176.6 (6)	C2—C5—C6—N6	−1.5 (13)
Cs1^{vii}—N2—C3—N3	−28.5 (7)	O3—N6—C6—N5	9.6 (11)
Cs2^{ix}—N2—C3—N3	101.4 (6)	O4—N6—C6—N5	−171.2 (7)
C1—C2—C3—N2	0.7 (7)	O3—N6—C6—C5	−170.2 (8)
C5—C2—C3—N2	−177.8 (6)	O4—N6—C6—C5	9.0 (11)

Symmetry codes: (i) −*x*+1, *y*−1/2, −*z*+2; (ii) −*x*, *y*−1/2, −*z*+1; (iii) *x*, *y*−1, *z*; (iv) *x*+1, *y*, *z*; (v) *x*, *y*, *z*−1; (vi) −*x*, *y*+1/2, −*z*+1; (vii) −*x*+1, *y*+1/2, −*z*+2; (viii) *x*, *y*+1, *z*; (ix) *x*, *y*, *z*+1; (x) *x*−1, *y*, *z*.

Hydrogen-bond geometry (Å, º)

D—H···*A*	*D*—H	H···*A*	*D*···*A*	*D*—H···*A*
O1*W*—H1*W*···N1^{vii}	0.85	2.01	2.855 (7)	171
O1*W*—H2*W*···N5^{vi}	0.85	2.50	3.334 (9)	168
C1—H1···O2^{iii}	0.94	2.83	3.508 (10)	130
C4—H4···O1^{xi}	0.94	2.62	3.547 (9)	168

Symmetry codes: (iii) *x*, *y*−1, *z*; (vi) −*x*, *y*+1/2, −*z*+1; (vii) −*x*+1, *y*+1/2, −*z*+2; (xi) −*x*, *y*−1/2, −*z*+2.